UNIVERSITY OF CALIFORNIA, SAN DIEGO

Nutrient Bioremediation by Algae and a Light Dependent Model for Predicting Algal Growth

A thesis submitted in partial satisfaction of the

requirements for the Degree Master of Science

in

Biology

by

Daniel P. Yee

Committee in Charge:

Professor B. Greg Mitchell, Chair
Professor James Golden, Co-Chair
Professor Julian Schroeder

2010

ProQuest LLC
789 East Eisenhower Parkway
P.O. Box 1346
Ann Arbor, MI 48106-1346

The Thesis of Daniel P. Yee is approved, and it is acceptable in quality and form for publication in microfilm and electronically:

_____

_____

Co-Chair

_____

Chair

University of California, San Diego

2010

I would like to dedicate this work to my parents, Lucy and Patrick, sister and brother-in-law, Joyclyn and Jay, and canines, Ginsu and Tati.

All of whose love and support bring joy and balance to my life.

TABLE OF CONTENTS

SIGNATURE PAGE iii
DEDICATION iv
TABLE OF CONTENTS v
LIST OF TABLES vii
LIST OF FIGURES viii
LIST OF ABBREVIATIONS ix
LIST OF SYMBOLS x
PREFACE xi
ACKNOWLEDGEMENTS xii
ABSTRACT OF THE THESIS xiii

CHAPTER 1: BIOREMEDIATION 1

ABSTRACT 1
1.1 INTRODUCTION 2
1.1.1 China's Water Quality and Resources 2
1.1.2 Phycoremediation and algal biotechnology 3
1.1.3 Assessing algal growth and nutrient removal 4
1.2 METHODS AND MATERIALS 5
1.2.1 Sample collection 5
1.2.2 Culture conditions 5
1.2.3 Measuring growth 6
1.2.4 Water quality analysis 6
1.2.5 Data analysis 6
1.3 RESULTS & DISCUSSION 8
1.3.1 Shanghai water quality 8
1.3.2 Growth of microalgae on polluted runoff 9
1.3.3 Nutrient removal efficiency 11
1.4 CONCLUSION 13

CHAPTER 2: MODELING GROWTH 15

ABSTRACT 15
2.1 INTRODUCTION 16
2.1.1 The marine diatom: Thalassiosira pseudonana 16
2.1.2 Algal biotechnology 17
2.1.3 Pigments 18
2.1.4 Modeling the growth of algae 19
2.2 METHODS AND MATERIALS 21
2.2.1 Culture conditions & Sampling 21
2.2.2 Chlorophyll-specific absorption coefficient 21
2.2.3 Specific growth rate, cell concentration, and sizes 22
2.2.4 Particulate carbon and nitrogen 22
2.2.5 Chlorophyll a and phaeopigments 22
2.2.6 HPLC pigments 22
2.2.7 In vitro absorption spectra 23
2.2.8 Quantum yields 23
2.3 RESULTS & DISCUSSION 24
2.3.1 Spectral irradiance 24
2.3.2 Pigmentation of Thalassiosira 24
2.3.4 Variation in $a^*_{ph}(\lambda)$ due to light limitation 25
2.3.5 Modeling chlorophyll specific absorption coefficient $a^*_{ph}(\lambda)$ 26

2.3.6 Modeling the chlorophyll to carbon ration (Chl a: C) 26
2.3.7 Observed Quantum yield for growth of Thalassiosira 26
2.3.8 Modeling quantum yield for growth 27
2.3.9 Modeling net growth rate (μ_n) 29
2.4 CONCLUSION 30

TABLES AND FIGURES 32

REFERENCES 54

LIST OF TABLES

Table 1. Analyzed macronutrients 33

Table 2. The U.S. EPA and China National Seawater Quality Standard (NSQS) water quality indexes 34

Table 3. Analyzed macronutrient in molar concentrations. 35

Table 4. Specific growth rates 36

Table 5. Nutrient removal efficiency 37

Table 6. Summary of growth, cellular, and photosynthetic characteristics for *Thalassiosira* 42

Table 7. Summary of the pigment profile 43

LIST OF FIGURES

Figure 1. Map of Shanghai and water sampling locations 38

Figure 2. Growth curves 39

Figure 3. DIN removal curves 40

Figure 4. DIP removal curves 41

Figure 5. Relative spectral irradiance 44

Figure 6. β-carotene per cell and composition of photosynthetic and photoprotective pigments 45

Figure 7. The in-vivo chlorophyll specific absorption spectrum 46

Figure 8. Mean HPLC and fluorometrically derived chlorophyll *a* per cell, and Cell diameter 47

Figure 9. The linear relationship between a^*_{ph} (436 and 676 nm) and light intensity 48

Figure 10. The linear fit between observed and estimated a^*_{ph} (436 and 676 nm) 49

Figure 11. The fit of observed Chl *a* to carbon ratio 50

Figure 12. The modeled light dependent quantum yield of growth 51

Figure 13. The linear fit between estimated and observed quantum yields 52

Figure 14. The predicted growth rates 53

LIST OF ABBREVIATIONS

OD	optical density
DIN	dissolved inorganic nitrogen
DIP	dissolved inorganic phosphorous
SH-1	Shanghai Sou Gang
SH-2	Bao Yang Wharf
SH-3	San Jia Gang
SH-4	Jin Shan In
SH-5	Jin Shan Out
NH_4	ammonia
NO_3	nitrate
NO_2	nitrite
PO_4	phosphate
Chl	chlorophyll
POC	particulate organic carbon
PON	particulate organic nitrogen
C	carbon
N	nitrogen
d	diameter of single cell (μm)
PS	photosynthetic pigments
PP	photoprotective pigments

LIST OF SYMBOLS

Δ_{cell}	nutrient removed per cell (fmol cell^{-1})
Δ_{cell}/t	nutrient removal rate per cell (fmol cell^{-1}d^{-1})
$\%\Delta$	total percent removal of nutrients
μ	specific growth rate (d^{-1})
μ_n	net growth rate (d^{-1})
λ	wavelengths (nm)
$E_0(\lambda)$	spectral quantum scalar irradiance (μmol quanta m^{-2} s^{-1})
PAR	photosynthetically available radiation defined as $\int_{400nm}^{700nm} E_0(\lambda)d\lambda$ (μmol quanta m^{-2} s^{-1})
$a^*_{ph}(\lambda)$	chlorophyll-specific absorption by phytoplankton (m^2 mg Chla^{-1})
ϕ_μ	quantum yield of growth (mol C fixed [mol quanta absorbed]$^{-1}$)
ϕ_m	maximal quantum yield (mol C fixed [mol quanta absorbed]$^{-1}$)
ϕ_{mEo}	maximal quantum yield at steady state irradiance (mol C fixed [mol quanta absorbed]$^{-1}$)
$E_{k\mu}$	saturation irradiance for growth (μmol quanta m^{-2} s^{-1})
μ_s^b	specific growth rate at optimal light intensity
α	initial slope for a non-linear fit
β	secondary slope for a non-linear fit

PREFACE

This thesis presents the study of several species of microalgae in order to elucidate patterns of growth, photosynthesis, and physiological efficiency under varying environmental conditions. The purpose of these studies is to support the application of microalgae for water remediation, biofuel production, and animal feed. As a part of forwarding progress in applications of algal biotechnology, strain selection and optimization of growing conditions is important for scale-up systems to be employed.

Chapter 1 is an assessment of water quality in Shanghai and lab studies of algal remediation of nutrient pollution. *Chlorella vulgaris* and *Isochrysis galbana* were grown at three temperatures using natural runoff as media for growth. Growth rates were determined as well as nutrient removal efficiencies of ammonia, nitrate, dissolved inorganic nitrogen, and dissolved inorganic phosphate for both species.

Chapter 2 describes a model for net growth rate for the marine diatom *Thalassiosira pseudonana* as a function of growth irradiance. Six cultures were grown under varying light intensities. Light dependent parameterizations of chlorophyll specific absorption, chlorophyll:carbon ratio, and quantum yields of growth are used in a spectrally integrated model for net growth rate.

ACKNOWLEDGEMENTS

All work presented in Chapter 1 was conducted in the lab of Peimin He at Shanghai Ocean University, and was funded in combination by National Science Foundation EAPSI program and the China Science and Technology Exchange Center. To study water quality and water-remediation using microalgae, culturing and analytical equipment, and strains of *Chlorella* vulgaris and *Isochrysis* galbana, were kindly provided by my hosts in the lab of Dr. He. Water samples from the Shanghai estuary were collected with the help Yang Wang, Zhi-hui Feng, and Jian-hung Zhang. I thank each and every one of them for welcoming me with open arms and helping me complete my experiments under relatively tight time constraints. I will not forget the kindness, hospitality, and fun times spent eating, debating, and playing Popkart!

Data from Chapter 2 was originally collected by Greg Mitchell, Maria Vernet, and Egil Sakshaug in 1986. I would like to thank Maria Vernet, whose keen memory and willingness in helping interpret this data set was invaluable.

I would like to thank everyone in the Scripps Photobiology Group, past and present, for providing me the framework for conducting my growth experiments. In particular: Brian Seegers, for being the backbone of the group (without you, I would not have been able to begin to fail); Ben Neal, who welcomed me into this madness; Brian Schieber, for his computer finesse; Mary Anderson, for her strength under pressure; lastly, Greg Mitchell, for his hands-off approach to allow me to struggle but develop into a stronger and more capable researcher.

ABSTRACT OF THE THESIS

Nutrient Bioremediation by Algae and a Light Dependent Model for Predicting Algal Growth

by

Daniel P. Yee

Master of Science in Biology

University of California, San Diego, 2010

Professor B. Greg Mitchell, Chair

This research focused on understanding the effects of microalgae on its environment at multiple scales. The first study examines algal growth in the context bioremediation. Eutrophic water from the Yangtze River Estuary and Shanghai coast was collected and used to culture *Chlorella vulgaris* and *Isochrysis galbana* at 15, 20, and 25°C under 58 μmol quanta m^{-2} s^{-1}. Nutrient removal by *Chlorella* did not vary between

temperatures with DIN removal rates ranging from 4.409 to 5.128 fmol cell^{-1} day^{-1} in SH-1, and 10.242 to 11.326 fmol cell^{-1} day^{-1} in SH-3. However, *Isochrysis* showed a temperature preference in which the 15°C culture and had a 3.5 to 3.8 fold decrease compared to 20 and 25°C in removal rates per cell, ranging from 0.605 to 2.328 fmol cell^{-1} day^{-1}. The second study parameterizes a mathematical model for the physiological processes of photosynthetic growth for the marine diatom, *Thalassiosira pseudonana.* Cultures of *Thalassiosira* were grown at 20°C at irradiances ranging from 31.4 to 1332 μmol quanta m^{-2} s^{-1}. The chlorophyll specific absorption at the blue peak, a^*_{ph} (436nm), increased from 0.017 to 0.049 m^2 mg Chla^{-1}, and for the red peak, a^*_{ph} (676 nm), from 0.013 to 0.024 m^2 mg Chla^{-1} with respect to increasing light intensity. Quantum yields for growth ranged from 0.016 to 0.081 mol C fixed [mol quanta absorbed]$^{-1}$. Specific growth rates, μ, ranged from 0.76 to 1.66 d^{-1}. Overall, the modeled results agreed well with observed values, but indicates the need to incorporate respiration for modeling net growth rate.

CHAPTER 1: BIOREMEDIATION

Abstract

Algae grown in nutrient-rich urban, industrial, and agricultural runoff holds great potential for water-remediation applications. In this study the effects of temperature and nutrients on the growth of freshwater algae *Chlorella vulgaris*, and marine algae *Isochrysis galbana* were investigated while grown in polluted surface runoff from the rivers and coasts of Shanghai. Pollution by nutrients were found to be moderately to very polluted according to China standards, and far exceeding the lower threshold set by U.S. EPA standards. Concentrations of ammonium, nitrate, DIN and DIP ranged from 0.035 to 0.094, 0.025 to 2.340, 0.094 to 3.462, and 0.007 to 0.065 mg L^{-1}, respectively. *Chlorella* grown in freshwater sources produced natural log growth rates ranging from 0.21-0.36 d^{-1}, while *Isochrysis* grown in a coastal water source produced growth rates ranging from 0.30-0.38 d^{-1}. Experiments were conducted for cultures grown at 15, 20, and 25°C under 58 μmol quanta m^{-2} s^{-1}. As expected, an inverse relationship between nutrient removal and growth was observed. In both species higher growth rates were achieved at 15°C but found to not be significantly different from other growth temperatures ($p>0.05$). Nutrient removal by *Chlorella* did not vary between temperatures with DIN removal rates ranging from 4.409 to 5.128 fmol $cell^{-1}$ day^{-1} in SH-1 and 10.242 to 11.326 fmol $cell^{-1}$ day^{-1} in SH-3. However, *Isochrysis* showed a temperature preference in that the 15°C culture and had a 3.5 to 3.8 fold decrease compared to 20 and 25°C in removal rates per cell, ranging from 0.605 to 2.328 fmol $cell^{-1}$ day^{-1}.

1.1 Introduction

1.1.1 China's Water Quality and Resources

China is a fast growing nation with much of its urban development occurring along the coast. In a review of China's water resources Varis and Vakkilainen (2001) concludes that an ever increasing population, urbanization, and uneven distribution of water, has led to each individual in China having less than half the water per person than in water-scarce countries such as Egypt. One of the eight issues Varis and Vakkilainen identify is the need for "environmental degradation to be reversed." One method for reversing the degradation of China's waters supply is through bioremediation.

Shanghai is one such overpopulated and urbanized city situated near the mouth of the Yangtze River. The Yangtze River is China's longest river, running 3,915 miles from the west and flows out to the East China Sea. In addition to significant traffic by large scale shipping, the estuary is also a catchment for anthropogenic inputs such as urban, industrial, and agricultural runoffs that empty out of the tributary Huangpu River. Over the past four decades nitrate Yangtze River has increase three fold and phosphate by 30% (Zhuo, Shen, and Yu 2007). When combined with favorable environmental conditions such as warm temperatures and high irradiance, eutrophic conditions often result in harmful algal blooms to occur. Harmful algal blooms as a result of eutrophication are common to the inner shelf of the East China Sea at the mouth of the Yangtze Rive, and peak during summer months (Chen et al. 2003).

1.1.2 Phycoremediation and algal biotechnology

Phycoremediation is defined as the use of macroalgae and microalgae for the removal or biotransformation of pollutants, including excess nutrients, from wastewater and CO_2 from waste air (Olguin 2003). Phycoremediation has long been studied for wastewater treatment and has proven to be an efficient method for treating human and animal wastes (Oswald 1957; McGarry and Tongkasame 1971; Groffman et al. 2003, Park 2009; Olguin et al. 2003). Phycoremediation has recently been explored as a method to deal with water pollution in China (He et al 2008; Yang et al. 2006). Many of these studies look at macroalgae species because there are easy to grow and harvest. So far these studies show promise that algae can effectively remove nutrients to improve water quality. In this study we consider the use of microalgae for bioremediation. Due to their small size and high surface area microalgae could potentially be faster in nutrient uptake and efficiency.

In addition to pollution mitigation, there is also interest in cultivating of algae on wastewater for products such as algal-protein and algal-biofuel (Olguin 2003; Woertz et al. 2009; Benemann et al. 2003). As energy costs rise and fossil fuel supplies become scarcer, research in the development of algal-biofuels has become an environmental and national security issue. With a potential demand for algal biomass, it would be mutually beneficial to grow algae in polluted or wastewater. Growing algae with waste nutrients and CO_2 would not only clean up the water but also provide a method for reducing cost by recycling nutrients from pollution to algae. Ideally, wastewater could provide all of the nutrients essential for algal growth.

1.1.3 Assessing algal growth and nutrient removal

If algae are to be used to remove nutrients and produce biomass, it is important to determine the optimal conditions for these goals to be achieved. Algae are photosynthetic organisms that thrive in all bodies of water and in all physical environments. Previous research on algae has studied the effects of different physical and nutrient limitation such as light, temperature, and nutrients on algal physiology. Some of the physiological responses studied are growth rates, absorption, photosynthesis, pigments, and biochemical variability (Sanchez et al. 2000; Herzig and Falkowski 1989; Moisan and Mitchell 1999). Algae's range of growth conditions is large, from -1.8°C in polar seawater to >45°C in thermal hot springs. Moisan and Mitchell (1999) have shown that *Phaeocystis antartica* can double its biomass in 3 days at 0°C with irradiances at less than 5% full sunlight.

Chlorella vulgaris and *Isochrysis galbana* are both well studied organisms in the laboratory. *C. vulgaris* is a chlorophyte commonly found in freshwater and nearshore ecosystems (Davis 1955) while *I. galbana* is a marine haptophyte commonly cultured as food for bivalves (Douillet and Langdon 1993)**.** In this study we observe the growth rates and nutrient removal efficiencies of *Chlorella vulgaris* and *Isochrysis galbana* grown at three temperatures in surface water was collected from several locations along the Yangtze River and Shanghai coast. Nutrient analysis was used to determine water quality as well as nutrient removal rates for experiments.

1.2 Methods and Materials

1.2.1 Sample collection

The locations where water was collected are shown in Figure 1. Sampling occurred during the month of July from three locations along the Shanghai portion of the Yangtze River; near a small river junction at Shanghai Sou Gang (SH-1: 31.416981, 121.485944), near the Huangpu River junction at Bao Yang Warf (SH-2: 31.407083, 121.497833), and near the coastal interface just east of Pudong International Airport at San Jia Gang (SH-3: 31.214411, 121.774167). Additionally, water was also collected at the coastal location at Jinshan beach, which is enclosed and contains treated ocean water that has been bioremediated by *Gracilaria verrucosa* (Huo 2010, submitted). Water was collected from inside (SH-4: 30.816494, 121.547992) and outside (SH-5: 30.816494, 121.547992) the bioremediated zone.

1.2.2 Culture conditions

Water from each location was filtered through 2 μm cellulosic membrane filters to remove debris and other microbial organism while leaving nutrients intact.

Cultures for inoculum were grown in 500 ml of f/2 medium (Guillard & Ryther 1962). Cell concentrations were calculated using a standard double chamber hemacytometer and Olympus light microscope. Cells from the inoculum were centrifuged and transferred to 250ml Erlenmeyer flasks containing 200ml of surface water from each respective location to achieve starting concentration of concentration of 5.0×10^5 cells ml^{-1}. Cultures were grown in GZX-300BS-III Shanghai CIMO Medical incubators under

12:12 h (L:D) cycle at 58 μmol qanta $m^{-2}s^{-1}$ using cool white fluorescent lamps, and temperatures set at 15°C, 25°C, and 30°C .

1.2.3 Measuring growth

Net specific growth rate (μ_n) was estimated by linear regression of $\log_e$-transformed determinations of optical density (OD). OD at 710 nm was measured in triplicate cultures every other day using a T6 New Century UV-Vis spectrophotometer. Earlier observations were used to generate a linear regression between cell counts and OD to estimate cell concentrations from OD. For *Chlorella*, the regression equation derived was: $y= 1*10^7x + 127614$, $R^2=0.921$, and for *Isochrysis* it was $y= 1*10^7x + 332280$, $R^2=0.897$.

1.2.4 Water quality analysis

Nutrients were analyzed four times over 16 days of growth. 15 ml culture and natural media were filtered through 2 μm cellulose membrane filters. The eluted media was immediately analyzed for NH_4, NO_3, NO_2, and PO_4 on a Skalar San++ Continuous Flow Analyzer (SA1050). Dissolved inorganic nitrogen (DIN) was calculated as the sum of NH_4, NO_3, and NO_2 while dissolved inorganic phosphorous (DIP) was a direct measurement of PO_4.

1.2.5 Data analysis

Nutrient removal per cell (Δ_{cell}) was calculated by taking the difference between nutrient concentrations divided by cell concentration during log-phase growth. Nutrient removal rates per cell (Δ_{cell}/t) were calculated by taking the difference between nutrient concentrations divided by the number of the days and cell concentration during log-

phase. One-way ANOVA was performed to test the differences in μ and Δ_{rate} across the three temperatures (α=0.05).

1.3 Results & Discussion

1.3.1 Shanghai water quality

Water from SH-1 contained the most inorganic nitrogen with NH_4, NO_3, NO_2 concentrations of 0.064, 2.075, and 1.323 mg L^{-1}, respectively (Table 1). Inorganic phosphorous was highest at SH-3 at 0.065 mg L^{-1} (Table 1). While SH-4 was originally sampled as a control site to demonstrate water quality of a remediated water source; surprisingly it was not the lowest in nutrients. Instead, SH-2 actually had the lowest nutrient concentrations of NH_4, NO_3, NO_2, and PO_4 at 0.035, 0.025, 0.076, and 0.031 μg L^{-1}, respectively. This is surprising because SH-2 is located at the junction of Shanghai's two manor rivers, the Huangpu and Yangtze.

In comparison to water quality indexes of China and the United States, the assessment of water quality varied. China's water quality standards comprise of five classification levels with quality worsening from I to V (Table 2). Ammonia and nitrate at all locations were all within level I standards. Nitrate at SH-1 was highest with level I classification, SH-3 and SH-4 were somewhere between level III and IV. DIN at SH-1 and SH-3 were the highest at level V followed by SH-4 classified between level III and IV, and SH-2 and SH-5. DIP concentrations for all locations were between level I and II except for SH-5 which was within level I standards. However, the U.S. EPA water quality index for nutrients is based on total dissolved inorganic nitrogen and dissolved inorganic phosphate and is much more stringent than its Chinese counterpart. In relation to U.S. EPA standards all sampled locations exceeded "low quality" DIN and DIP concentrations of 1.0 and 0.1 mg L^{-1}, respectively.

Nitrogen is widely accepted to be the main limiting nutrient in marine ecosystems. As nitrogen pollution is greatest where agricultural activity and urbanization occur (Howarth and Marino 2006), algal standing stock in the Yangtze estuary has increased over the past four decades, resulting in about 30 to 80 red tide events occurring between 2000 to 2005 (Zhuo et al 2007). While NH_4 in runoff has increased from animal wastes and fertilizers, NO_3 was the largest contributor to DIN in our samples. The concentration of NO_3 ranged from 0.41 to 33.34 μmol L^{-1} while NH_4 ranged from 1.94 to 5.21 μmol L^{-1}. While the proportions of nitrate to ammonia are consistent with findings for the Yangtze River by Liu et al. (2003), the magnitude of the concentrations are generally lower than most locations in their study. Nevertheless, nutrient analyzed during this study are capable of supporting high algal production with SH-1, SH-3, and SH-4 having DIN close to eutrophic levels as described by Chai et al (2006).

1.3.2 Growth of microalgae on polluted runoff

Following pretreatment, all samples of *Chlorella* grown in SH-2 and *Isochrysis* in SH-5 failed following 6 days of incubation. Several reasons for the collapse of the cultures were considered, including bacterial contamination, chemical toxicity from metals or herbicides, and insufficient nutrients. In a study by Yoshida et al. (2004), it was found that the nitrogen quota for *C. vulgaris* to be 0.239 pg $cell^{-1}$. Based on this figure and cell concentrations of our cultures, it was determined that SH-2 only had 33% of the required nitrogen to support cell growth. Therefore, insufficient nitrogen was identified as the cause of culture death in SH-2, despite not having a full nutrient profile the same was assumed for SH-5. The rest of this study focuses on cultures grown in water from the remaining three locations (SH-1, SH-2, and SH-3) which all had high amounts of DIN.

Table 4 summarizes the specific growth rates, μ, and cell concentrations during log-phase growth at the three locations. The highest μ was observed in cultures of *Isochrysis* grown in water from SH-4, from 0.3 to 0.38 d^{-1}, in order of decreasing temperature. It is unusual to see μ decrease with increasing temperature since metabolic activity normally declines at colder temperatures in most living organisms. However, the final biomass of *Isochrysis* accumulated at 15°C by the end of this study was about 25% lower than at both 20 and 25°C (Figure 2C). Though *Isochrysis* was observed to achieve a faster specific growth rate, its final biomass was observed to be lower than those of *Chlorella* grown in water from SH-1 and SH-3.

Between SH-1 and SH-3, neither produced higher specific growth rates for *Chlorella*, however, SH-3 did achieve slightly higher final concentrations in biomass for all three temperatures (Figure 2B). The trends for the growth in water from SH-3 are very similar, which indicates that under the given nutrient concentrations at this location *Chlorella* is insensitive to changes in temperature. However, *Chlorella* grown in water from SH-2 was sensitive to temperature, with the final concentration at 15°C about 30% less than at 20 and 25°C (Figure 2A).

Despite observed differences in specific growth rate, ANOVA testing indicated that μ across the three temperatures were not significantly different ($p>0.05$). In comparison to other studies on the effects of temperature on *Chlorella*, μ increased linearly with temperature, with rates ranging from 0.182 to 0.463 d^{-1} (Mayo 1997). Other studies have observed *Isochrysis* with a wide range of μ from 0.18 to 1.32 d^{-1}. In regards to the higher growth rate at lower temperature, it is possible that *Isochrysis* increases its

physiological activity under stressful conditions, such as low light and temperature, in order to compete for nutrients.

1.3.3 Nutrient removal efficiency

In this study, we define efficiency of nutrient removal in three ways. First is nutrient removed per cell (Δ_{cell}), then the nutrient removal rate per cell (Δ_{cell}/d), and lastly, the total percent removal of nutrients (%Δ), all during log-phase growth. In Table 5, we provide the three nutrient removal efficiency parameters for nitrate, ammonia, DIN, and DIP.

We begin by comparing removal of nitrate and ammonia. In general, algae preferred nitrate over ammonia as a nitrogen source. In seven out of nine cultures %Δ for nitrate ranged from 82.9 to 99.4%, while ammonia ranged from very low at 1.3%, moderately low 30.9%, and moderately high at 81.2%. The cellular removal, Δ_{cell}, ranges from 6.460 to 27.9 fmol cell^{-1} for nitrate and 0.021 to 2.9 fmol cell^{-1} for ammonia. The uptake of nutrients depends on the availability of nutrients. Energetically speaking, ammonia would be the more energetically efficient nutrient to use because it can be immediately used without being further reduced. However, because ammonia levels in our water were very low compared to nitrate, both *Chlorella* and *Isochrysis* in most conditions may have acclimated their nitrogen uptake for the more abundant nutrient, nitrate.

To compare nutrient removal among temperatures, we combine the removal nitrate, nitrite, and ammonia into one as DIN. DIN removal per cell was higher in *Chlorella* grown in water from SH-1 over SH-3. The Δ_{cell} for SH-1 and SH-3 ranged from 17.636 to 20.512 and 10.242 to 11.362 fmol cell^{-1}, respectively (Table 5). As we can see,

there is not much distinction in DIN removal between temperatures, even amongst the removal rates, Δ_{cell}/d, which ranged from 4.409 to 5.128 and 2.561 to 2.832 fmol cell^{-1}d^{-1}, respectively. Both cellular removal and removal rate of DIN match well with the specific growth rates, showing a correlative trend, and further verifying the importance of nitrogen uptake on growth. However the correlation between growth and nutrient removal is scattered for *Isochrysis* grown in water from SH-4. Temperature sensitivity was exhibited in the 15°C culture, in which the Δ_{cell}/d showed a 3.5 to 3.8 fold decrease compared to removal rates at 20°C and 25°C. This might explain why the final biomass concentration of *Isochrysis* at 15°C was lower.

DIP was present in much lower levels and did not show much variation in Δ_{cell} or Δ_{cell}/d. Δ_{cell} in all nine conditions ranged from 0.083 to 0.205 fmol cell^{-1}, while Δ_{cell}/d ranged from 0.008 to 0.021 fmol cell^{-1}d^{-1}.

In this study *Chlorella* grown in water from SH-3 removed a maximum of 94% and 85% of NO_3 and PO_4, respectively, while *Isochrysis* grown in SH-4 removed a maximum of 99% and 65% of NO_3 and PO_4, respectively. All of these results combined indicate that *Chlorella* and *Isochrysis* hold potential to be organisms used for bioremediation purposes.

1.4 Conclusion

The Yangtze River is known to be one of the busiest waterways in all of China, with Shanghai as a hub for development and industry, there is a constant flux of nutrients and pollutions in these waters. The surface water quality of macronutrients in the Yangtze River during July of 2009 would be classified as moderately polluted. In all five locations sampled, the DIP did not exceed level II China's national standard, while DIN covered all five levels, with three of five locations classified as level V. In comparing to US EPA standards, DIN and DIP far exceed the low quality index.

In a study by Wu (2005), the dissolved inorganic nitrogen (DIN) and inorganic phosphorous (IP) were analyzed at locations similar to ours along the Yangtze estuary and assessed for their mutagenic activity. The results show that locations with the highest mutagenic activity had DIN and IP concentrations as high as1.84 mg L^{-1} and 0.047 mg L^{-1}. These concentrations are similar to levels found at SH-1 and SH-3, which during this study had DIN of 1.032 mg L^{-1} and 0.839 mg L^{-1}, and IP of 0.553 μg L^{-1} and 0.687 μg L^{-1}, respectively. This indicates that in addition to creating a eutrophic environment, the nutrients may also be harming marine life directly by causing mutations.

Of the two actively uptaken sources of nitrogen, NO_3 contributed to the highest amount of nutrient removed in both species. While NO_3 removal was high in both organisms, both species had varied affinities for NH_4 uptake. This affinity of nitrate over ammonium is inconsistent with findings by Valenzuela-Espinoza et al. (1999), in which NO_3 uptake by *I. galbana* grown in an agricultural fertilizer media was low until NH_4 was

exhausted in the media. We explain that our observation maybe due to acclimatization of nitrogen uptake for nitrate when ammonia concentrations are low.

It was observed that nitrate is the limiting macronutrient for the growth of both species. Other micronutrients such as vitamins and metals important for overall growth and health should be analyzed for a more thorough study. Temperature did not exhibit a significant difference on growth and removal rates. These results imply that *C. vulgaris* and *I. galbana* have a wide optimal temperature range between 15°C-25°C for growth. From a bioremediation point of view, this evidence that either species would be suitable for outdoor growing during Shanghai's spring and fall seasons, when temperatures range average between 15°C-25°C.

This study shows that nutrient levels in Shanghai's runoff were able to sustain dense growth of microalgae. *C. vulgaris* and *I. galbana* were two species that showed potential for nutrient remediation. Current in situ studies of algae remediation in China use macroalgae due to the ease in which their biomass can be harvested (He et al. 2008; Huo et al. 2010) However, due to its planktonic qualities, using microalgae in open systems could be detrimental to the natural environment. Instead, we suggest microalgal potential in closed systems, such as in algal ponds or bioreactors, where polluted and wastewater could be used as nutrients to support algae cultivation for biotechnology.

CHAPTER 2: MODELING GROWTH

Abstract

Models of growth and production of algae are important for predicting changes in algal communities in the environment, as well as in ponds and bioreactors for commercial cultivation. In this study we aimed to create a predictive model for the growth, quantum yield, and spectral absorption of *Thalassiosira. pseudonana* acclimated to a varying light environment. Cultures of *T. pseudonana*, a marine diatom which holds potential for biotechnological applications in biofuel production was grown at six light levels ranging from 31.4 to 1332 μmol quanta m^{-2} s^{-1}. This study modeled chlorophyll specific absorption, Chl *a*: C, quantum yields for growth, all parameterized based on growth irradiance. These modeled properties were integrated it into a model for net growth rate of *Thalassiosira*. The chlorophyll specific absorption at the blue peak, a^*_{ph} (436nm), increased linearly from 0.017 to 0.049 m^2 mg $Chla^{-1}$, and for the red peak, a^*_{ph} (676 nm), from 0.013 to 0.024 m^2 mg $Chla^{-1}$ with respect to increasing light intensity. Quantum yields for growth were observed to range from 0.016 to 0.081 mol C fixed [mol quanta absorbed] $^{-1}$. Specific growth rates, μ, were observed at 0.76 to 1.66 d^{-1}. Overall, the results of our model agreed well with observed values, but indicate the need to incorporate respiration for modeling net growth rate

2.1 Introduction

2.1.1 The marine diatom: *Thalassiosira pseudonana*

A simple description of algae would be that they are photosynthetic organisms that account for 45% of the world's primary production (Falkowski and Raven 2007). Microalgae in particular can be thought of as single celled plants that share many similarities to that of higher-land plants. Microalgae are fast growing unicellular phytoplankton that are primary producers in the aquatic food chain and influence carbon and nitrogen cycles in the world's lakes and oceans. Because of this, the presence of microalgae across the world's aquatic environments is often used to indicate sites of ecological and biogeochemical significance. Phycologists have long been fascinated by the role of algae as primary producers in all aquatic environments and have spent decades researching the mechanisms and physical conditions that effect algal growth.

Bacillariophyceae are a class within the phylum Heterokonktophyta, and are commonly referred to as diatoms. Diatoms play a significant role in marine ecology and dominate the oceans across various spatial and temporal seasons. Diatoms are known to be bloom forming and account for over 40% of the primary production in the sea (Nelson 1995). With approximately five-thousand known marine species, many studies have been done to try to explain their ecological success. One of the most unique features ubiquitous to all diatoms is their ability to synthesize microscopically intricate silicate outer cell walls called frustrules. The hard silicate is also thought to increase efficiency of nutrient uptake and provide protection from predators and the environment. Due to their

dependence on silica, diatoms have been found to dominate the Southern Ocean, where sediments are higher in siliceous elements (DeMaster 1979).

Thalassiosira pseudonana is a marine centric diatom and is one the few species that has recently had its entire genome (nuclear, plastid, and mitochondrial) sequenced with findings published by Armbrust et al (2004). This makes *T. pseudonana* a unique organism to study because it's physiological and biochemical phenotypes can now be traced to specific sequences in its genes to better understand metabolic pathways. With a reported ability to accumulate more than 70% of its biomass as polar lipid under certain physiological conditions (Brown et al. 1996) *T. pseudonana* is one of many organisms being studied for algal-derived biofuels.

2.1.2 Algal biotechnology

Many studies have been published on the effects of physical and chemical conditions including, light, temperature, nutrients, and pH on the growth of marine phytoplankton (Rhee and Gotham 1981; Falkowski 1985). Generally, these studies look at the effect these conditions have on efficiency of growth and photosynthesis. Other studies also look at nutrient kinetics (Olson et al. 1980), and biochemistry of amino acids, pigments, lipids, proteins, and carbohydrates (Brown et al 1996; Valenzuela-Espinoza 2007).

Studying these effects is important for defining ecological success of microalgae as well as conditions required for commercial algae cultivation. Applications of large scale cultivation include algal derived food, biofuel, and nutraceuticals. Traditional nutraceuticals include agar and carrageen used as thickening agents in food. Higher value medical products include probiotic supplements, anti-cholesterol, antiviral, anticancer,

and anticoagulant agents (Fitton et al. 2008). An application with large social and economic impact is the development of biofuels from algae. Recent interest and investment approaches $1 billion a year globally in this technology, and has been funded through governments and venture capital with hopes of producing a reliable alternative to fossil fuels. However, this process has proven to be costly. Current economic models project that the cost of a barrel algal-biofuel to be $1-2000 compared to less than $100 per barrel of fossil petroleum. Therefore, before any product can be commercially produced, algae cultivation has to become more economical. One way to do this is to be able to predict the conditions needed for optimized growth of a species. Ultimately, just as for terrestrial crops, different strains will be developed in different seasons and regions.

2.1.3 Pigments

A major field in the study of algal biology is the role of pigments and their composition in different species. The relationship between pigments and photosynthesis subsequently influence the optical physiology of algae. In addition to photosynthesis, pigments also aid in photoprotection. The photosynthetic apparatus is subject to damage through photooxidative stress by routine donation of electron to oxygen during photosynthesis or UV damage. The photosynthetic mechinery must be routinely maintained (Foyer et al. 1994). Certain protective pigments, xanthophylls and carotenes, can dissipate excess photons flux through vibrational heat release, reducing the amount of damage incurred. For *Thalassiosira* the photoprotective pigments are diatoxanthin, diadinozanthin, and β-carotene. Mycosporine amino acids are water soluble UV absorbing compounds that are believed to minimize UV damage (Moisan and Mitchell

2001). The photosynthetically active pigments in the light harvesting complex of diatoms comprises of a 25 kD protein are chlorophyll a, chlorophyll c, fucoxanthin, and a minor group of fucoxanthin derivatives (Friedman et al. 1984). The pigment abundance and ratios are species specific and vary in relation to physical conditions. Variations in cellular pigment concentrations compared to physiological parameters such as carbon, absorption, and quantum yields provides information about the physiological activity in the cells.

2.1.4 Modeling the growth of algae

Most phycology research has been motivated by goals to understand the ocean, coastal, estuarine, and freshwater ecology. A major aspect of this effort is to be able to estimate primary production in the natural environment. However, as interest in algae cultivations increase, similar studies in controlled systems may prove to be relevant in industry as well.

The specific growth rate is the time rate of change in biomass (e.g. rate of production per unit of biomass). For algae, growth is dependent largely upon, light, temperature, and nutrients. Early work by Jassby and Platt (1976) aimed to find mathematical formulations for fitting photosynthesis versus irradiance curves of set the stage for modeling phytoplankton growth. At the beginning of the 1980s, researches began to model cell growth in relation to photon absorption (Laws and Bannister 1980; Falkowski et al. 1985; Kiefer and Mitchell 1983; Sakshaug and Andresen 1989).

Net growth (μ_n) in algae is defined as the sum of the specific rate of dark respiration and specific growth rate. An accurate model must account for both of these parameters. When growing fast, respiration accounts for a small percentage of μ_n and

like most models we have not measured respiration for our final product. Instead, we propose a model following the methods of Moisan and Mitchell (1999) that predicts net growth rates as a function of growth irradiance.

Like many contemporary models (Moisan and Mitchell 1999; Sakshaug and Andresen 1989) we utilize the chlorophyll-specific spectral absorption coefficient $a^*_{ph}(\lambda)$ and quantum yield of growth ϕ_μ as photophysiological parameters in models of growth,

$$\mu_n = \frac{Chla}{C}\int_{400nm}^{700nm} a^*_{ph}(\lambda)E_0(\lambda)\phi_\mu d\lambda \quad \textbf{Equation 1}$$

Equation 1 is a spectral model within the visible range of wavelengths, where μ_n is the net growth rate, E_o is the spectral scalar irradiance, *Chl a:C* is the chlorophyll *a* and carbon concentration, and Φ_μ is the quantum yield of growth. Following typical methods, absorbed photons are estimated as the integral from 400 to 700 nm (photosynthetically active radiation, PAR). Moisan and Mitchell (1999) have shown photosynthetic activity was capable down to 300 nm using fluorescent spectroscopy. The illumination system used here had minimal irradiance below 400 nm as the lower limit. In order to parameterize the net growth rate of algal species that hold potential for commercial cultivation and understand physiological mechanisms that control variables within models, the absorption characteristics and photophysiological growth parameters $a^*_{ph}(\lambda)$ and ϕ_μ for *Thalassiosira pseudonana* have been characterized in the laboratory and estimated for modeling.

2.2 Methods and Materials

2.2.1 Culture conditions & Sampling

Cultures of *Thalassiosira psuedonana* (Hustedt Hasle and Heimdal, clone 3H) was grown in GPM medium in six 4 L Pyrex glass bottles. Five of the bottles were wrapped with screens and illuminated by cool white fluorescent lights to achieve 5 irradiance levels, the sixth and highest irradiance was achieved by illumination under a halogen spotlight. Average irradiance was measured for all six bottles with a 4 pi sensor (Biospherical Instruments) and estimated to be 41.4, 48.8, 118, 552, 858, 1332 μmol-quanta m^{-2} sec^{-1}. All the cultures were incubated in a 20°C water-bath.

Cultures were inoculated to give an initial Chl *a* concentration of 1-2 μg L^{-1} and growth was monitored with in vivo fluorescence twice daily. Cultures reached exponential growth after 10 days and were maintained in log-phase growth by diluting with fresh media in 1:3-1:1 dilution ratios. Cultures were sampled during log-phase growth to generate three replicate experiments over consecutive days. During experimental days cell counts, cell size, fluorometric chlorophyll, HPLC pigments, POC/PON, and cellular absorption were measured for various analyses.

2.2.2 Chlorophyll-specific absorption coefficient

In vivo whole cell absorption was determined at 1 nm intervals using a dual beam spectrophotometer. For this 5 to15ml of culture was filtered on GF/F filters and measured for relative absorption. GPM media was used as a reference and blank. The chlorophyll-specific absorption coefficient was estimated by dividing $\log_e$ absorption, $a_{ph}(\lambda)$, by a corresponding mean fluorometric and HPLC Chl *a* value,

$$a^{*}_{ph}(\lambda) = a_{ph}(\lambda)\,[\text{chl } a]^{-1}. \quad \textbf{Equation 2}$$

2.2.3 Specific growth rate, cell concentration, and sizes

Specific growth rate (μ) was estimated by linear regression of $\log_e$-transformed determinations of in vivo fluorescence on a fluorometer, sampled twice daily. Cell counts were done on a Sedwig-Fadtig hemacytometer for each culture and day of experiment. 50 ml of culture was preserved with Lugols and kept dark for microscopy and cell measurements. Cell size was measured with a grated ocular micrometer at 200, 400, or 1,000x magnification depending on cell size. Cell volume was determined by assuming a spherical cell with the diameter measured.

2.2.4 Particulate carbon and nitrogen

Intracellular carbon and nitrogen (POC/PON) were measured by gas chromatography. 20 ml of culture were filtered onto Whatman GF/F filters, dried at 90°C overnight, and frozen until analysis.

2.2.5 Chlorophyll a and phaeopigments

Samples were prepared by filtering 5 ml of culture onto 2.5 cm Whatman GF/F filters and extracted in 10 ml of MeOH. The extracts were centrifuged until clear, Chl *a* and phaeopigments were measured on a Turner Designs fluorometer following the method of Reimann and Holm-Hansen (1978).

2.2.6 HPLC pigments

Chlorophylls and carotenoids were measured by high performance liquid chromatography. Aliquots of 50 and 100 ml were filtered on 2.5 cm Whatman GF/F filters and extracted with 3ml of 90% acetone for 24 h. A reverse-phase stepwise gradient

elution system with 3 HPLC grade solvents was employed: 90:10 MeOH; water (v/v). 94.6 MeOH:water (v/v), and 100% MeOH at a rate of 1ml min^{-1}. The water in the first solvent contained an ion-pairing reagent (Mantoura and Llewellyn 1983) in concentrations of 1.5g tetrabutylammonium and 0.96g of ammonium acetate per 100ml of water.

Pigments were separated in a C-18 Econosphere column from Alltech with 5 μm particles and dimensions of 4.3 mm x 25 cm. The column was calibrated with pure pigments obtained by injecting different volumes of an extract of known concentration. For this purpose, pigments were extracted from different unialgal cultures, isolated by thin-layer chromatography (Guillard and Lorenzen 1972), dissolved in solvent, identified by its visible absorption spectrum, and quantified using the corresponding specific absorption coefficients. Pigment concentration was calculated by manually measuring the corresponding peak area.

2.2.7 In vitro absorption spectra

Absorption spectra of individual treatments were reconstructed by using individual pigment spectra scaled to the estimated pigment concentration. Spectrum of individual pigments were obtained after separation of the pigments on a C-18 column (as described above) with the outflow connected to a Hitachi Spectrophotometer Model U-2000 fitted with a flow-through cell.

2.2.8 Quantum yields

Quantum yield for growth was based on the carbon specific growth rate, the whole cell in vivo spectral absorption, and the spectral irradiance in each treatment (Sosik and Mitchell 1991, 1995)

2.3 Results & Discussion

2.3.1 Spectral irradiance

Figure 5 shows the relative spectral irradiance curves for both light sources, with the halogen lamp having a gradual increase followed by a decrease at around 589 nm. The spectrum of the fluorescent lights had three major peaks, the first at 441 nm, then 550 nm, and lastly, 589 nm. Each curve represents the relative spectral photosynthetically available radiation (PAR).

2.3.2 Pigmentation of *Thalassiosira*

The pigment profile elucidated by HPLC is important because it affects the spectral shape of $a^*_{ph}(\lambda)$. The pigments and pigment concentrations analyzed were consistent to those found in *T. pseudonana* by Mas et al. (2008). The photosynthetic pigments comprised of chlorophyll *a*, chlorophyll *c*, fucoxanthin, β-carotene, and minor chromatogram peak from a fucoxanthin derivative. When combined, these pigments made up 81 to 97% of the pigments per cell (Table 7). Normally, β-carotene is considered to be a photoprotective pigment, but here, it was observed to increase with decreasing light intensity along with the other photosynthetic pigments (Figures 6A, B). The photoprotective pigments were identified to be diadinoxanthin and diatoxanthin which accounted for 2 to 18% of total pigments per cell depending on incubation irradiance (Table 7). Photosynthetic pigments decreased exponentially from 0.591 to 0.085 pg cell^{-1}, while photoprotective pigment concentration stayed relatively constant across light intensities ranging from 0.0151 to 0.0196 pg cell^{-1}(Figure 6B).

2.3.4 Variation in $a^*_{ph}(\lambda)$ due to light limitation

The chlorophyll specific absorption of *Thalassiosira* varied under the different growth irradiances, and increased linearly with light intensity (Figure 7). While cultures acclimated to lower light intensities have more cellular chl *a* (Figure 8A), they are also subject to more self shading which lowers their optical-absorption cross section (Berner et al. 1989). Additionally, cells with more chlorophyll have thicker thylakoid stacks, resulting in pigment packaging effect which also decreases absorption per chlorophyll. This decrease in optical-absorption cross section diminishes with an increase in cell diameter and subsequently cell size which was observed in *Thalassiosira* (Figure 8B).

Figure 9 shows that the chlorophyll specific absorption increases linearly at both the blue peak, a^*_{ph} (436 nm), from 0.017 to 0.049 m^2 mg $Chla^{-1}$, and for the red peak, a^*_{ph} (676 nm), from 0.013 to 0.024 m^2 mg $Chla^{-1}$ with respect to increasing light intensity. These two peaks reflect the wavelengths at which Chl *a* absorbs the most photons of light. The chlorophyll specific absorption found here are consistent to observed ranges of 0.018 to 0.23 for *T. pseudonana* (Mitchell and Kiefer 1988) and 0.014 to 0.025, in related species, *T. weisflogii* (Dubinsky et al. 1986).

The ratio of a^*_{ph} (436 nm) to a^*_{ph} (676 nm) also show a linear increase from 1.35 to 1.99 with respect to light intensity (Table 6). This trend is due to a smaller-fold increase in the red absorption band compared to the blue band with increasing light intensity. This observation is visualized in the chlorophyll specific absorption spectrum (Figure 7), where at low light, the relationship between red peaks show a 1.8 fold decrease versus a 2.8 fold increase in the blue peaks. Bricaud et al. (1995), attributes similar relationships in absorption changes to pigment packaging.

2.3.5 Modeling chlorophyll specific absorption coefficient $a^*_{ph}(\lambda)$

From the observed chlorophyll specific absorption coefficient $a^*_{ph}(\lambda)$ was modeled at each nm wavelength. An example of this is shown in Figure 4A, which plots the linear fits of a^*_{ph}(436 nm) and a^*_{ph}(676 nm) across the spectrum of light intensity. From these fits, a^*_{ph} was estimated at 436 and 676 nm at our growth irradiances. Figures 10A and B show the linearity between our estimated and observed values for a^*_{ph}(436 nm) and a^*_{ph}(676 nm), R^2= 0.95 and 0.85, respectively.

The fits were expressed by the simple equation for a line: $y=mx+b$, with y representing the chlorophyll specific absorption, x as the growth irradiance, while m and b were parameterized by the fitted line.

2.3.6 Modeling the chlorophyll to carbon ratio (Chl a: C)

The modeling of Chl *a*: C was performed by plotting observed Chl *a*: C over growth irradiances and finding an equation to fit the data (Figure 11A). The equation for the fitted data is,

$$\text{Chl } a\text{: C} = 0.3939E_o^{-0.5018}. \qquad \textbf{Equation 3}$$

The estimated values were plotted versus observed values in Figure 11B, and show a good linear fit with R^2= 0.99.

2.3.7 Observed Quantum yield for growth of Thalassiosira

Quantum yield of growth, ϕ_μ, is an essential variable in bio-optical modeling of net growth rate, μ_n. Modeled estimates of photosynthesis are very sensitive to variability in quantum yield (Sosik 1996). From the rearrangement of Equation 1, quantum yield of growth is represented as,

$$\phi_{\mu} = \frac{\mu_n}{Chl : C \int_{400nm}^{700nm} a^*_{ph}(\lambda) E_0(\lambda) d\lambda} \qquad \textbf{Equation 4}$$

The observed ϕ_{μ} from this study ranged from 0.016 to 0.081 mol C (mol quanta absorbed)$^{-1}$. The trend for ϕ_{μ} shows a short increase followed by an exponential decline with increasing light intensity at 118 μmol quanta m^{-2} s^{-1} (Figure 12).

While respiration occurs in all cells, the observed ϕ_{μ} at 31.4 and 48.8 μmol quanta m^{-2} s^{-1} were subject to more respiration at low light. Respiration is an oxidative process that consumes oxygen and evolves carbon dioxide to supply ATP and carbon skeletons for biosynthesis (Falkowski and Raven 2007). Because the light intensity was below saturation, respiration increases to maximize its energy production.

At light intensities above 118 μmol quanta m^{-2} s^{-1} quantum yields begin to decease as a result of non-photochemical quenching via the diatoxanthin cycle. As the PAR exceeds the saturating level, ϕ_{μ} declines because excess photons are dissipated as heat in order to prevent photooxidative damage in the photosystem. This is supported in our observations that diatoxanthin and diadinoxanthin, remain relatively constant at all light intensities.

2.3.8 Modeling quantum yield for growth

Previous models for quantum yield for photosynthesis have been modeled with the product of maximal quantum yield, ϕ_m, which is obtained from short term P-E relationships (Sakshaug et al 1989). The method by Moisan and Mitchell (1999) excludes ϕ_m in exchange for an environmentally dependent maximal quantum yield, ϕ_{mEo}. They reason that the ϕ_m from short term P-E experiments are in over-idealized conditions and

do not reflect the maximum quantum yield for a given environment. Their equation for light dependent ϕ_μ is expressed as,

$$\phi_\mu = \phi_{mE_o,T} \frac{1-\exp^{-E_o/E_{k\mu}}}{E_o/E_{k\mu}} \qquad \textbf{Equation 5}$$

However, when this approach was applied we found values for ϕ_{mEo} above the theoretical maximum (ϕ_m =0.125). Instead we substitute ϕ_{mEo} with the theoretical maximum and express Equation 4 as,

$$\phi_\mu = 0.125 \frac{1-\exp^{-E_o/E_{k\mu}}}{E_o/E_{k\mu}} \quad \textbf{Equation 6}$$

.

A non-linear curve fitting equation by Platt et al. (1981) was modified to fit observed specific growth rates, μ,

$$\mu_n = \mu s^b [1-\exp(\frac{-\alpha PAR}{\mu s^b})] * \exp(\frac{-\beta PAR}{\mu s^b}) \qquad \textbf{Equation 7}$$

The curve was used to calculate the saturation irradiance for growth, $E_{k\mu}$. The parameters for Equation 6 were estimated and the maximum specific growth rate ($\mu_s{}^b$) initial slope (α) ,and secondary slope (β) were 1.934, 0.0352, and 0.0059, respectively. The fitted curve is shown is Figure 13B was used to calculate a $E_{k\mu}$ of 96 µmol quanta $m^{-2}s^{-1}$.

With the parameter for $E_{k\mu}$ defined we were able to predict ϕ_μ a full range of light intensities up to 1400 µmol quanta m^{-2} s^{-1} (Figure 12). Figure 13A shows the linear fit between observed and predicted quantum yields of growth, R^2= 0.7082. The lack of fit is mostly due to a decrease in ϕ_μ by respiration at low light, which was not captured in this model.

2.3.9 Modeling net growth rate (μ_n)

Finally, with $a^*_{ph}(\lambda)$, Chl *a*: *C*, and ϕ_μ parameterized, we integrate each model into the equation for net growth rate, repeated here,

$$\mu_n = \frac{Chla}{C}\int_{400nm}^{700nm} a^*_{ph}(\lambda)E_0(\lambda)\phi_\mu d\lambda \,. \quad \text{(Equation 1, repeated)}$$

The predicted μ_n are plotted alongside observed values in Figure 14. The trends are similar, showing an initial increase to a maximum net growth rate, followed by a decline as light intensity continues into saturating levels. Again we test the model against observed μ_n and find that they agree with an R^2 of 0.58. The flaw in our model is the overestimation of μ_n at low light. In our three lowest light levels, the overestimation shows 1.12 to 1.77 fold increase with decreasing irradiance. Again, the overestimation is traced back to the uncharacterized respiration. Since our modeled quantum yields of growth over predicts at low light intensity, this gets carried over into the model for μ_n, as well. However, this was to be expected, and the difference between observed and predicted μ_n at least gives us an idea of the relative amount of respiration at each light intensity. Although the net growth model remains to be improved to include respiration, it did accurately predict the trend and μ_n at higher irradiances where respiration is minimal.

2.4 Conclusion

By studying algae in a dynamic light environment we were able to model the absorption, Chl *a* to carbon, quantum yield of growth, and net growth rates of using a single parameter of irradiance. This basic study of algae biology could lead to greater implications for the environment and algal biotechnology. In comparison to oceanographic models our model was parameterized using idealized conditions, with similar models have been applied to estimate growth in the natural environment. However, it may prove evenmore useful for suggesting growth conditions for monocultures cultivated for aquaculture feedstock, biofuels, or nutraceuticals derived from algae. For example, if investors wanted to build an outdoor algae pond raising *Thalassiosira*, we could project the growth rates using daily PAR measurements specific to that region and season.

However, a resounding problem in most growth models is the lack of information on respiration rate. Previous experiments have been done to measure the respiration rate of Thalassiosira (Burris 1977; Parker and Armbrust 2004). Many models either neglect the role of respiration or substitute predicted rate to correct their models (Sakshaug et al 1989). However, in another study, Sakshaug et al (1991) improved their previous model by measuring respiration in cultures of *Thalassiosira nordenskioeldii* and *Chaetoceros furcellatus*. Rates were very low for most cultures and ranged from 11-56% of growth rate.

For our studies, further research should first parameterize respiration. This would very likely improve the R^2 values between observed and estimated quantum yields for

growth, and net growth rates. Additionally, real, species specific maximum quantum yields should be obtained for the estimation of ϕ_μ to further increase the accuracy of our model.

TABLES AND FIGURES

Table 1. Analyzed macronutrient weight concentrations (mg L^{-1}), with respective China quality level in parenthesis, for the five water locations SH-1, SH-2, SH-3, SH-4, and SH-5 in July 2009.

	SH-1	SH-2	SH-3	SH-4	SH-5
NH_4	0.064 (I)	0.035 (I)	0.052 (I)	0.094 (I)	0.094 (I)
NO_3	2.075 (I)	0.025 (I)	2.34 (I)	1.586 (I)	-
NO_2	1.323 (IV)	0.076 (II)	0.511(III-IV)	0.108 (III-IV)	-
DIN	3.462 (V)	0.136 (1)	2.903 (V)	1.788 (IV-V)	0.094 (I)
DIP	0.053 (V)	0.031(II)	0.065 (I)	0.030(I-II)	0.007 (I)

-: Data unavailable

Table 2. The U.S. EPA and China National Seawater Quality Standard (NSQS) water quality indexes; highest to lowest quality (left to right) in mg L^{-1}

	U.S.			China				
	High	Moderate	Low	Level I	Level II	Level III	Level IV	Level V
NH_4	-	-	-	0.15	0.50	1.00	1.50	2.00
NO_3	-	-	-	10.00	10.00	10.00	20.00	25.00
NO_2	-	-	-	0.06	0.10	0.15	1.00	1.00
DIN	0.5	0.5-1.0	1	0.20	0.50	1.00	1.50	2.00
DIP	0.01	0.01-0.1	0.1	0.02	0.10	0.20	0.30	0.40

-: Data unavailable

U.S. index is from the National Coastal Condition Report II. U.S. EPA (2004)

NO_2 index is from GB3838 (1988), NO_3 index is from GHZB1 (1999), all other China indexes are from GB3838 (2002)

Table 3. Analyzed macronutrient in molar concentrations (μmol L^{-1}) for the five water locations SH-1, SH-2, SH-3, SH-4, and SH-5 in July 2009.

	SH-1	SH-2	SH-3	SH-4	SH-5
NH_4	3.55	1.94	2.88	5.21	5.21
NO_3	33.47	0.41	37.74	25.57	-
NO_2	28.76	1.65	11.11	2.35	-
DIN	65.77	4.00	51.73	33.13	-
DIP	0.56	0.33	0.68	0.32	0.08

-: Data unavailable

Table 4. Specific growth rates, μ, and cell counts during log-phase growth of *Chlorella* (SH-1 and 3) and *Isochrysis* (SH-4) grown at 15, 20, and 25°C at 58 μmol quanta m^{-2} s^{-1}.

	SH-1			SH-3			SH-4		
	15°C	20°C	25°C	15°C	20°C	25°C	15°C	20°C	25°C
μ (d^{-1})	0.33	0.27	0.34	0.36	0.21	0.34	0.38	0.34	0.30
cells ml^{-1}	2.80E+06	3.34E+06	3.51E+06	4.35E+06	4.65E+06	3.79E+06	1.30E+06	9.10E+05	1.10E+06

-: Data unavailable

Table 5. Nutrient removal efficiency in femto-moles of concentration of removal per cell, molar rate of removal per cell, and percent removal of nitrate, ammonia, DIN, and DIP during log-phase growth by *Chlorella* cultured in water from SH-1 and SH-3 and *Isochrysis* cultured in water from SH-4 at 15, 20, and 25°C under a light intensity of 58 µmol quanta m^{-2} s^{-1}.

		SH-1			SH-3			SH-4		
		15°C	20°C	25°C	15°C	20°C	25°C	15°C	20°C	25°C
Nitrate	Δ_{cell}	6.487	6.460	7.890	12.667	10.266	8.927	7.623	27.943	-
	Δ_{cell}/t	1.622	1.615	1.972	3.167	2.567	2.232	0.762	2.794	-
	%Δ	84.4	89.7	89.3	94.0	90.7	82.9	38.9	99.4	-
Ammonia	Δ_{cell}	0.021	0.223	0.756	0.429	0.476	0.011	1.232	2.132	2.924
	Δ_{cell}/t	0.005	0.056	0.189	0.107	0.119	0.003	0.308	0.533	0.731
	%Δ	2.6	29.3	81.2	41.9	55.5	1.3	30.9	37.2	61.7
DIN	Δ_{cell}	20.512	18.106	17.636	11.065	10.242	11.326	6.048	23.285	21.496
	Δ_{cell}/t	5.128	4.526	4.409	2.766	2.561	2.832	0.605	2.328	2.150
	%Δ	87.4	91.8	94.1	93.1	92.0	83.0	23.8	63.9	71.3
DIP	Δ_{cell}	0.157	0.083	0.125	0.135	0.124	0.155	0.160	0.205	0.122
	Δ_{cell}/t	0.016	0.008	0.013	0.013	0.012	0.015	0.016	0.020	0.012
	%Δ	79.5	49.9	79.5	85.2	84.1	85.3	65.5	58.4	42.2

-: Data unavailable

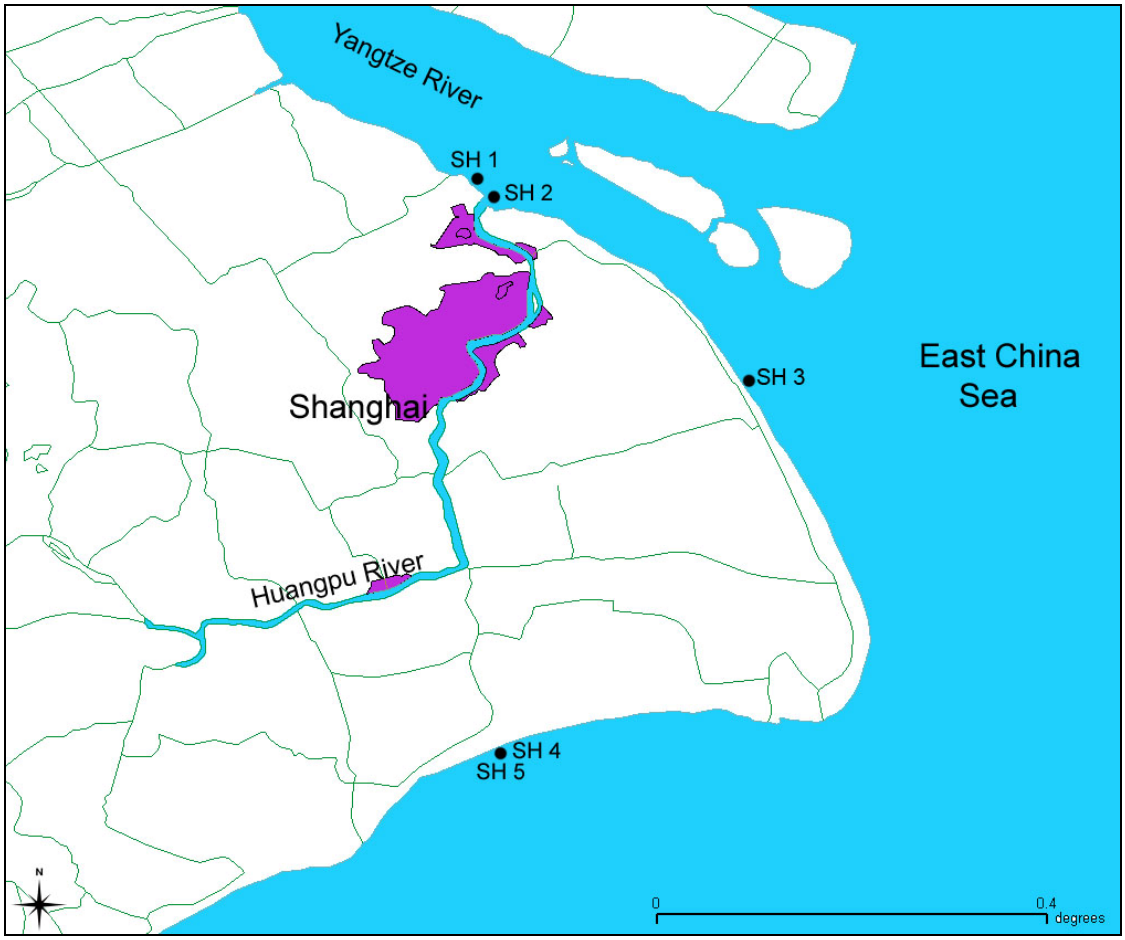

Figure 1. Map of Shanghai and water sampling locations along the Yangtze River mouth and Shanghai Coast (SH-1, SH-2, SH-3, SH-4, and SH-5)

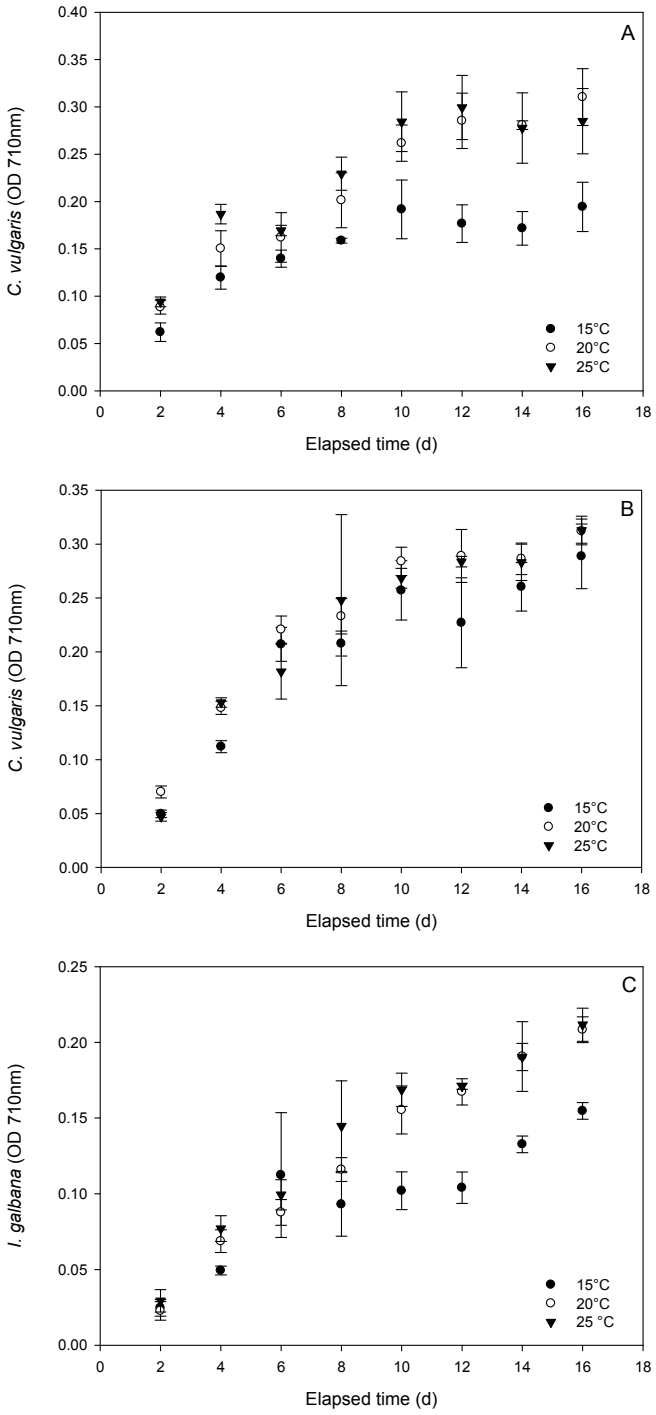

Figure 2. Growth curves of (A) *Chlorella* cultured in water from SH-1 (B) SH-3, and (C) *Isochrysis* cultured in water from SH-4 at 15, 20, and 25°C under a light intensity of 58 µmol quanta m^{-2} s^{-1}.

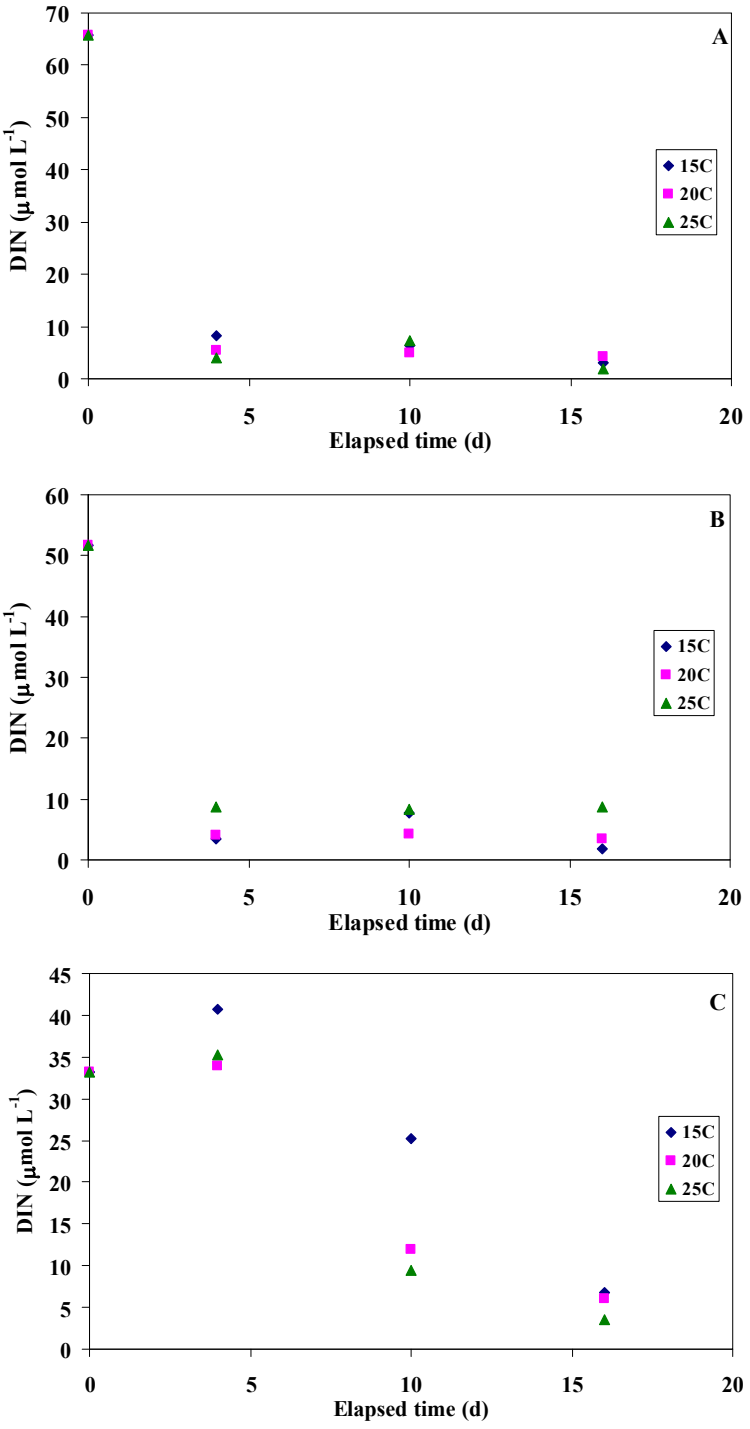

Figure 3. DIN removal curves of (A) *Chlorella* cultured in water from SH-1 (B) SH-3, and (C) *Isochrysis* cultured in water from SH-4 at 15, 20, and 25°C under a light intensity of 58 µmol quanta m^{-2} s^{-1}.

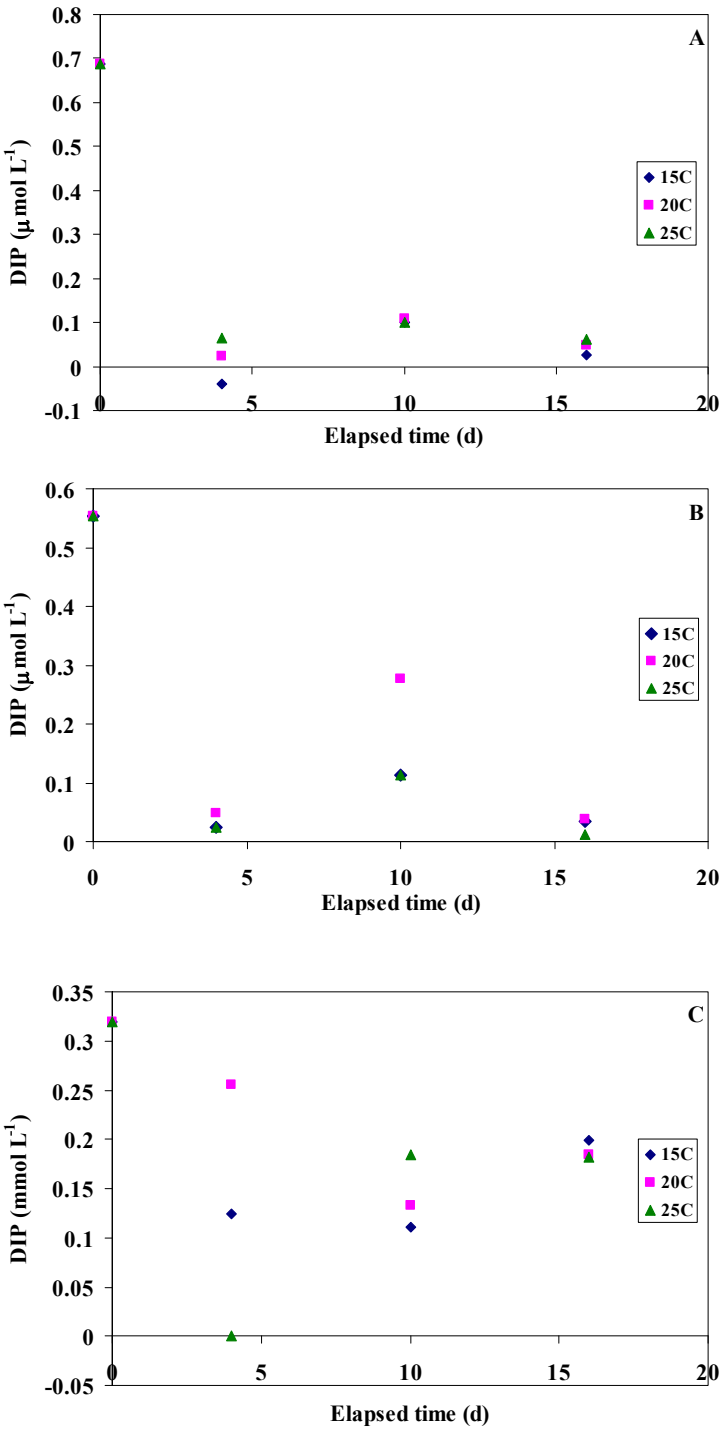

Figure 4. DIP removal curves of (A) *Chlorella* cultured in water from SH-1 (B) SH-3, and (C) *Isochrysis* cultured in water from SH-4 at 15, 20, and 25°C under a light intensity of 58 µmol quanta m^{-2} s^{-1}.

Table 6. Summary of growth, cellular, and photosynthetic characteristics for *Thalassiosira* grown at 20°C under six irradiances during steady-state conditions.

	Irradiance (μmol quanta m^{-2} s^{-1})					
	31.4	48.8	118	552	858	1332
μ (d^{-1})	0.76	1.19	1.66	1.66	1.44	1.33
Chl *a*:C ratio (w:w)	0.009	0.015	0.018	0.035	0.057	0.067
C:N ratio (w:w)	6.56	7.66	7.43	8.99	9.98	9.74
pg Chl a $cell^{-1}$	0.40	0.29	0.21	0.11	0.08	0.06
a^*_{ph} (436 nm)	0.018	0.024	0.025	0.034	0.038	0.049
a^*_{ph} (676 nm)	0.013	0.018	0.017	0.021	0.022	0.025
(436:676 nm)	1.36	1.36	1.48	1.68	1.69	2.00
$\Phi\mu$	0.054	0.071	0.081	0.029	0.019	0.016

Table 7. Summary of the pigment profile, concentrations (pg cell^{-1}), and ratios for *Thalassiosira* grown at 20°C under six irradiances under steady-state conditions. The photosynthetic pigments (PS) are chlorophyll a, c, fucoxanthin, and unidentified fucoxanthin derivative. The photoprotective pigments (PP) comprise of β-carotene, diadinoxanthin (DD), and diatoxanthin (DT). The mean Chl *a* was calculated by average fluorometric and HPLC results, and are used in calculations for estimating photosynthetic characteristics. Only HPLC values were used for comparing pigment ratios.

Light intensity μmol quanta m^{-2} s^{-1}	Chl a									Total pigment	PS	PP	Fraction of total pigment (w:w)	
	Fluor	HPLC	Mean	Chl c	Fuco	$Fuco_{deriv}$	B-carot	DD	DT	per cell	per cell	per cell	PS	PP
31.4	0.393	0.400	0.396	0.021	0.150	0.0072	0.0123	0.0151	0.0000	0.606	0.591	0.0151	0.975	0.025
48.8	0.278	0.296	0.287	0.023	0.128	0.0055	0.0089	0.0162	0.0000	0.478	0.462	0.0162	0.966	0.034
118	0.217	0.208	0.213	0.013	0.092	0.0045	0.0077	0.0175	0.0000	0.343	0.325	0.0175	0.949	0.051
552	0.105	0.114	0.109	0.011	0.049	0.0017	0.0029	0.0158	0.0028	0.197	0.178	0.0186	0.906	0.094
858	0.088	0.071	0.080	0.008	0.035	0.0013	0.0025	0.0145	0.0030	0.136	0.118	0.0175	0.871	0.129
1332	0.066	0.052	0.059	0.004	0.025	0.0010	0.0021	0.0155	0.0041	0.105	0.085	0.0196	0.812	0.188

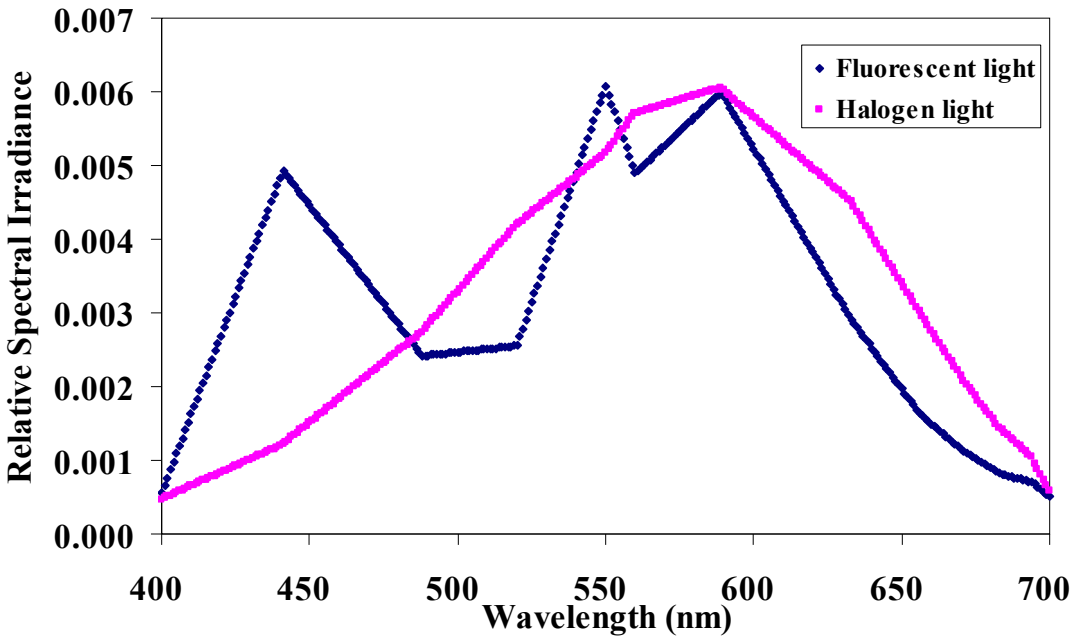

Figure 5. Relative spectral irradiance of the fluorescent and halogen lights used in growth incubators. The spectra are normalized so that the sum of the spectrum adds to 1.0.

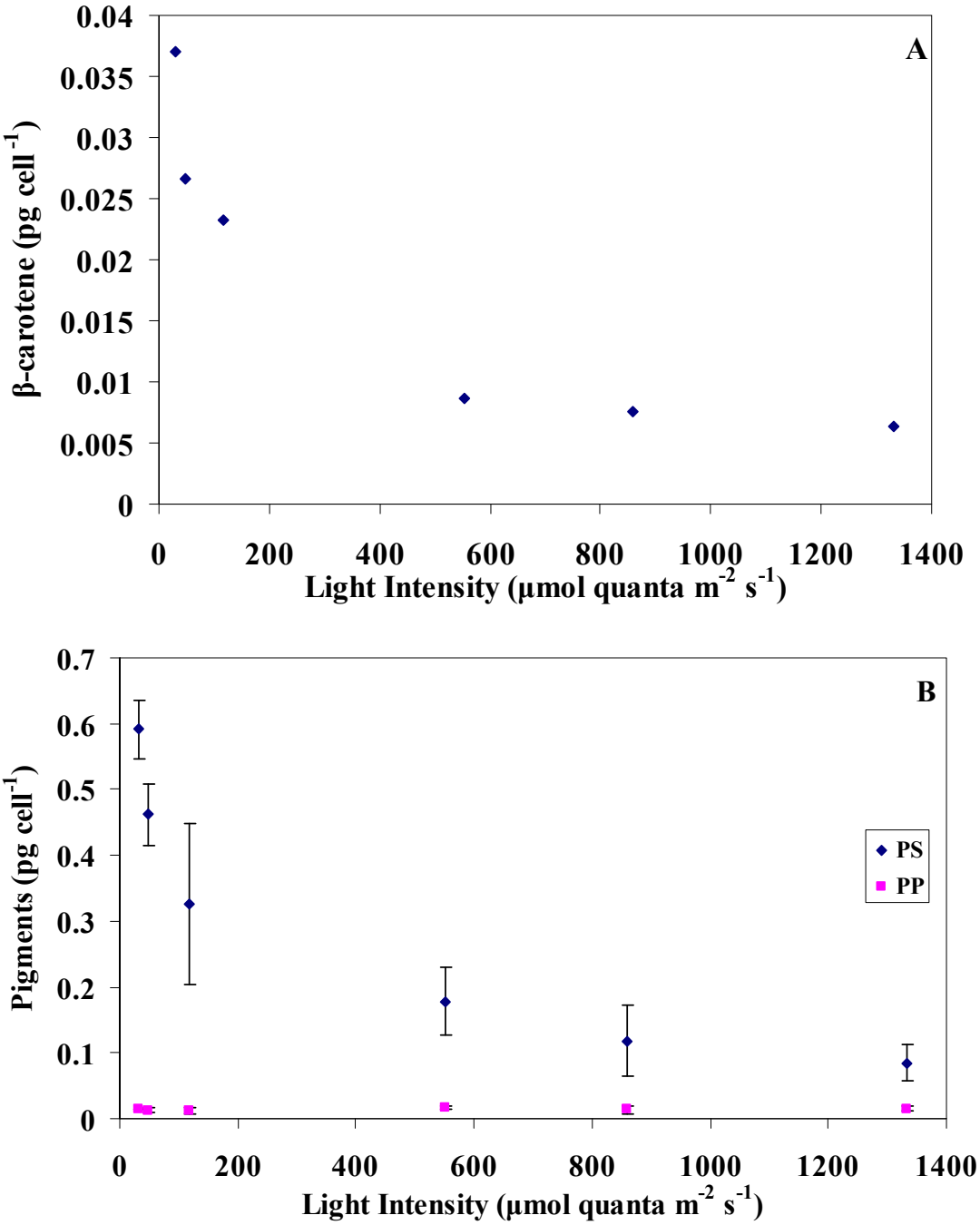

Figure 6. β-carotene per cell and composition of photosynthetic and photoprotective pigments. (A) β-carotene per cell and (B) composition of photosynthetic (PS) and photo-protective (PP) pigments per cell and for *Thalassiosira* grown between 31.4 and 1332 μmol quanta m^{-2} s^{-1} at 20°C under steady-state conditions.

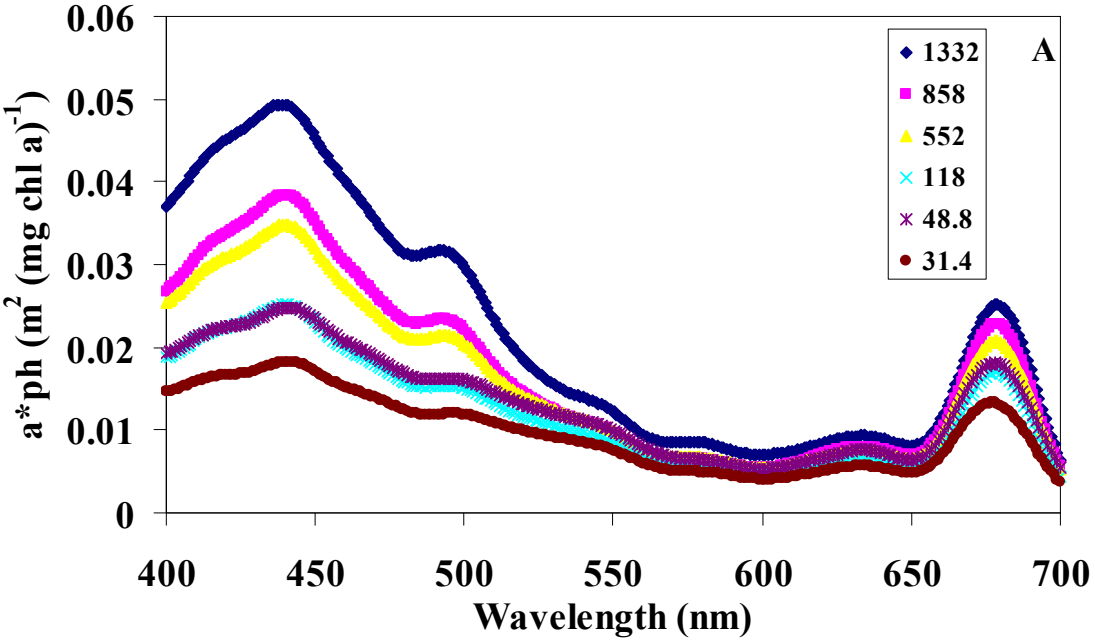

Figure 7. The in vivo chlorophyll specific absorption spectrum. (A) The in-vivo chlorophyll specific absorption spectrum for *Thalassiosira* grown between 31.4 and 1332 μmol quanta m^{-2} s^{-1} at 20°C under steady-state conditions.

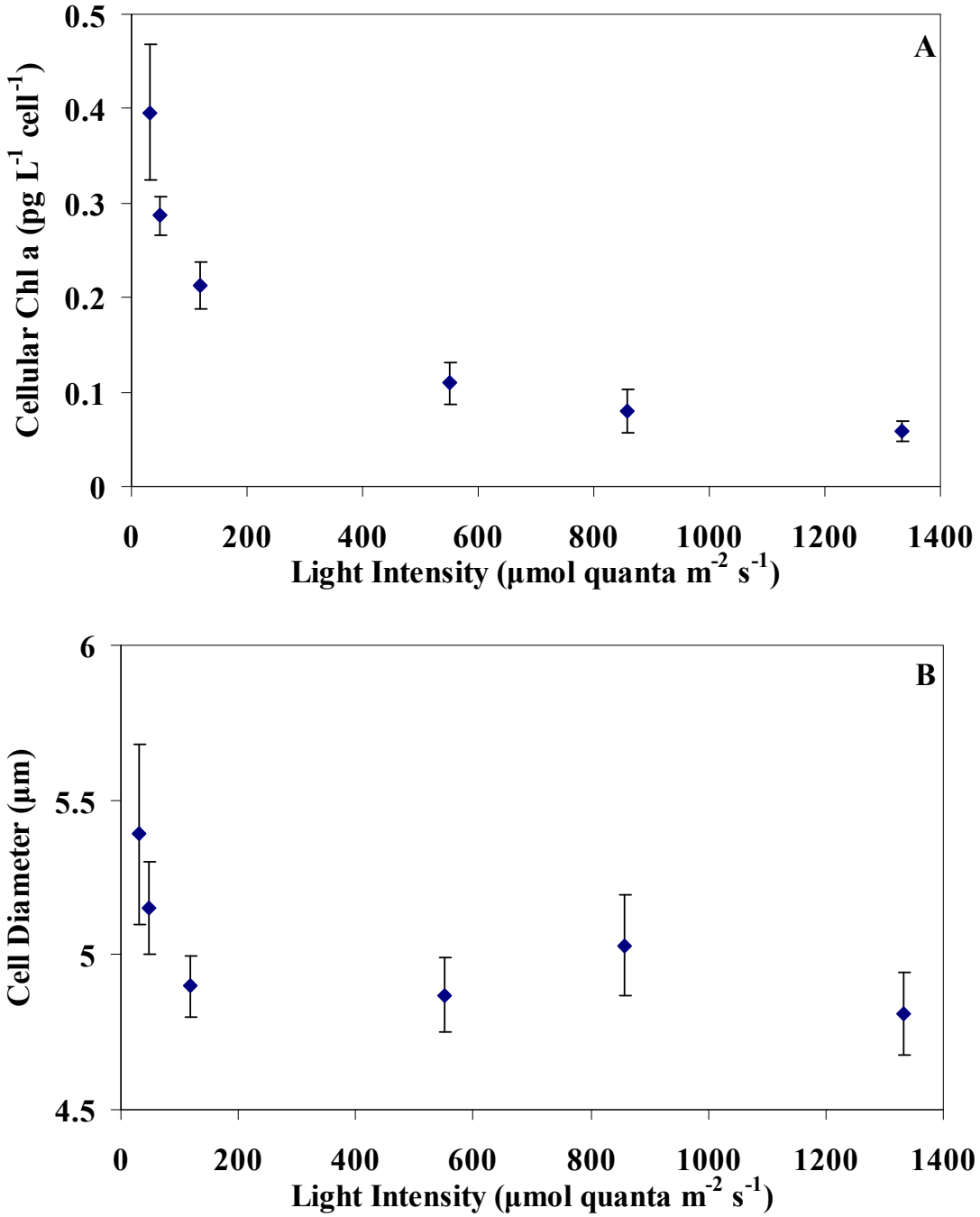

Figure 8. Mean HPLC and fluorometrically derived chlorophyll *a* per cell, and Cell diameter. (B) Mean HPLC and fluorometrically derived chlorophyll *a* per cell, and (C) Cell diameter for *Thalassiosira* grown between 31.4 and 1332 *µ*mol quanta m^{-2} s^{-1} at 20°C under steady-state conditions.

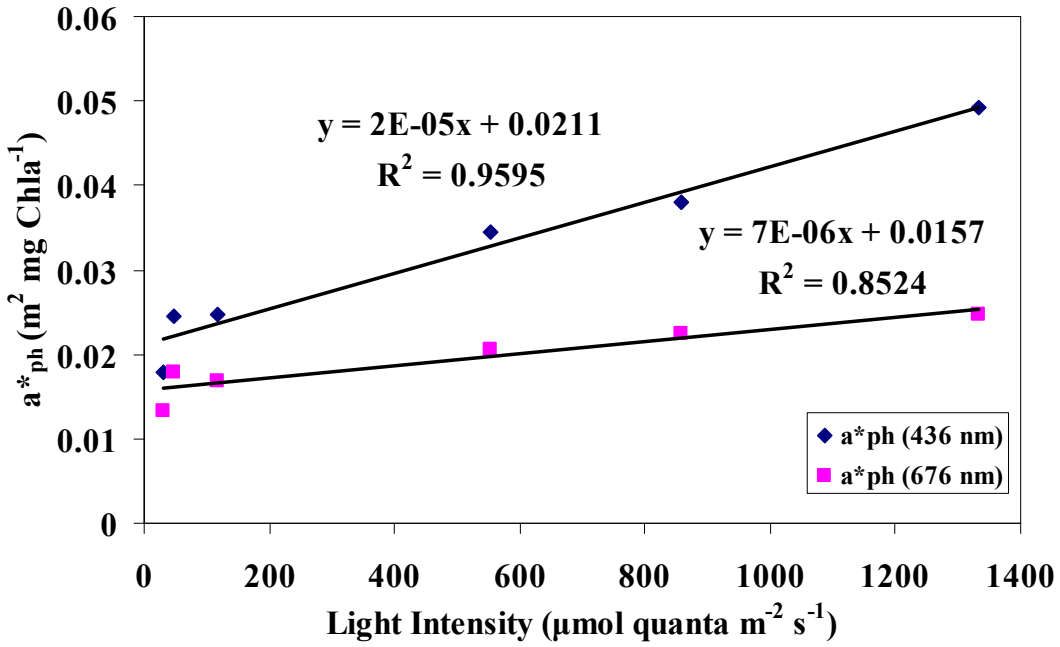

Figure 9. The linear relationship a^*_{ph} (436 and 676 nm) and light intensity for *Thalassiosira* grown between 31.4 and 1332 μmol quanta m^{-2} s^{-1} at 20°C under steady-state conditions.

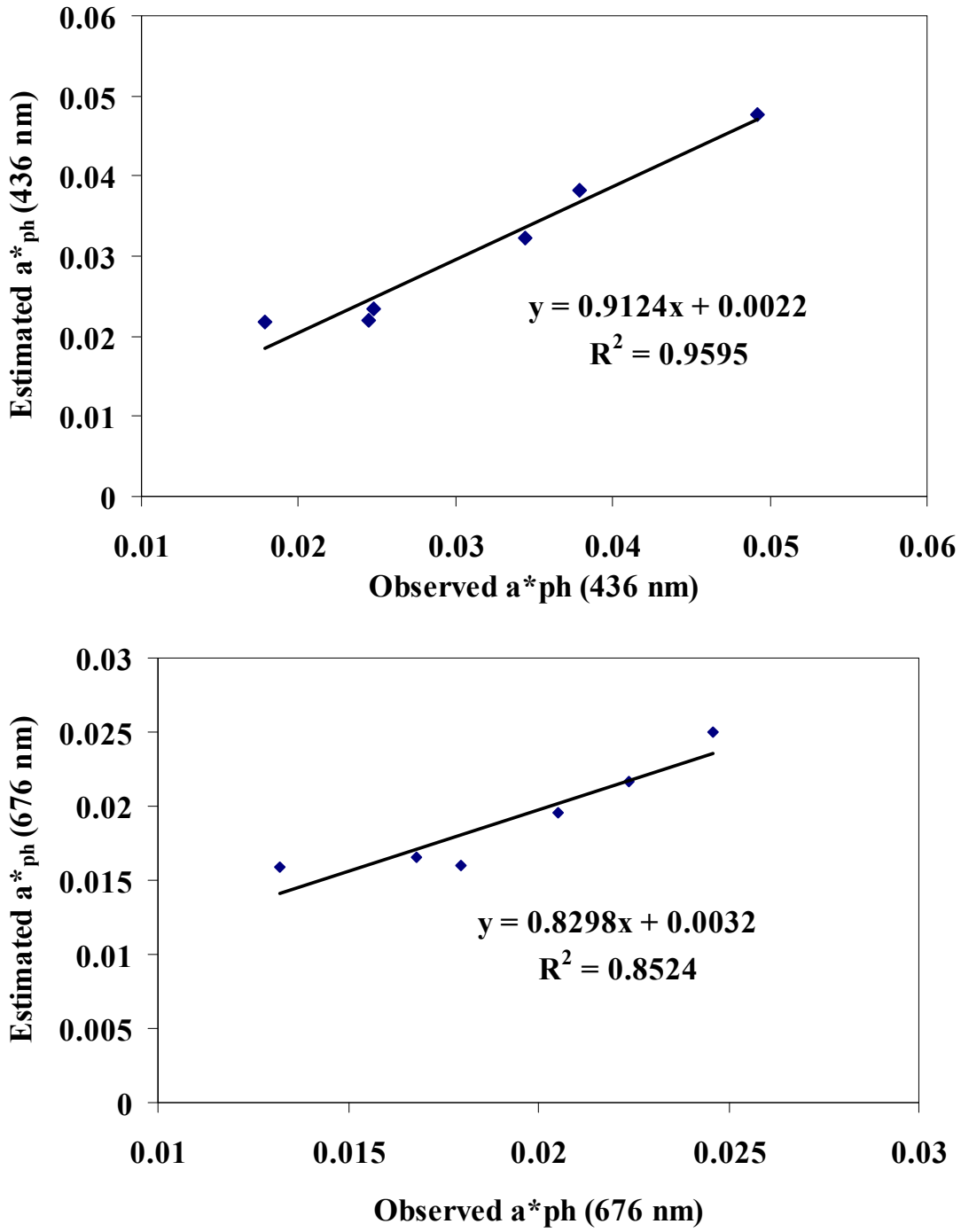

Figure 10. The linear fit between observed and estimated a^*_{ph} (436 and 676 nm). (A and B) The linear fit between observed and estimated a^*_{ph} (436 and 676 nm) for *Thalassiosira* grown between 31.4 and 1332 μmol quanta m^{-2} s^{-1} at 20°C under steady-state conditions.

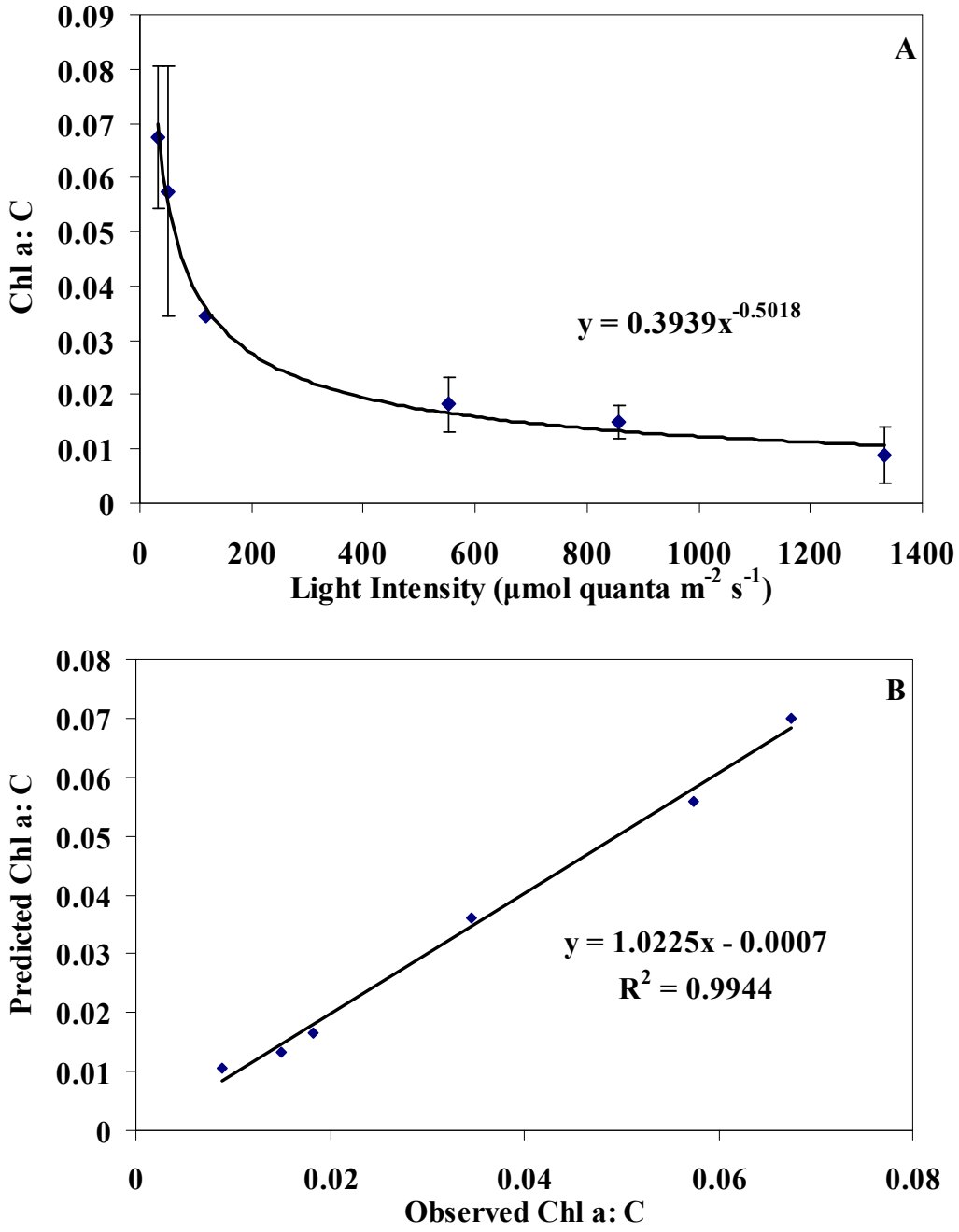

Figure 11. The fit of observed Chl *a* to carbon ratio (A) and the linear fit between predicted and observed Chl *a*: C (B) for *Thalassiosira* grown between 31.4 and 1332 *µ*mol quanta m^{-2} s^{-1} at 20°C under steady-state conditions

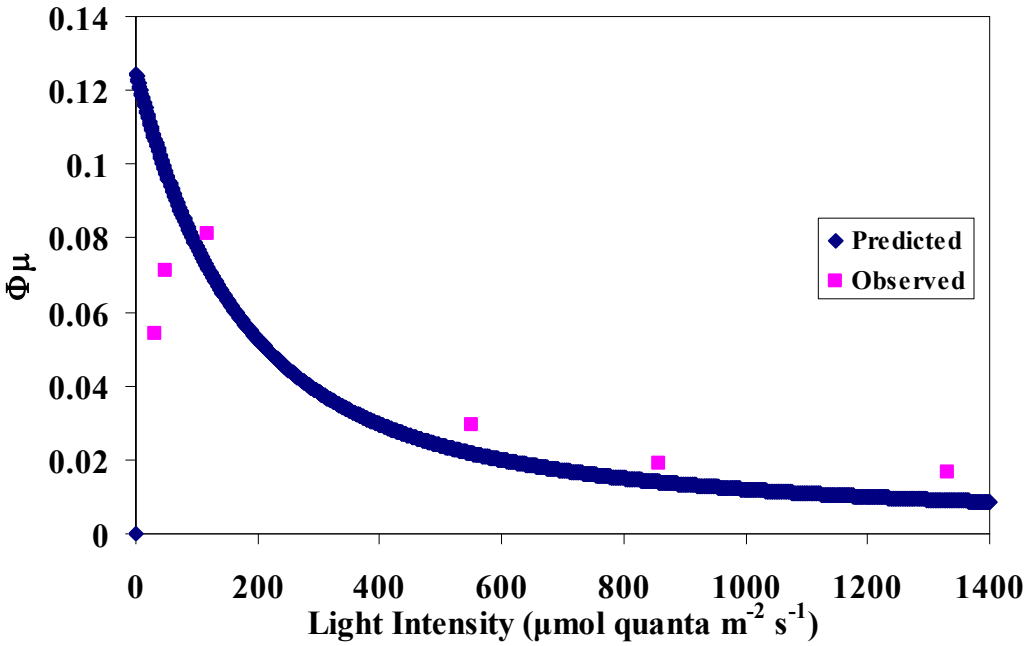

Figure 12. The modeled light dependent quantum yield of growth ϕ_{μ} for *T. pseudonana* using equation 6 calculated with $E_{k\mu}$= 96 μmol quanta m^{-2} s^{-1} and ϕ_{m} = 0.125, alongside observed values.

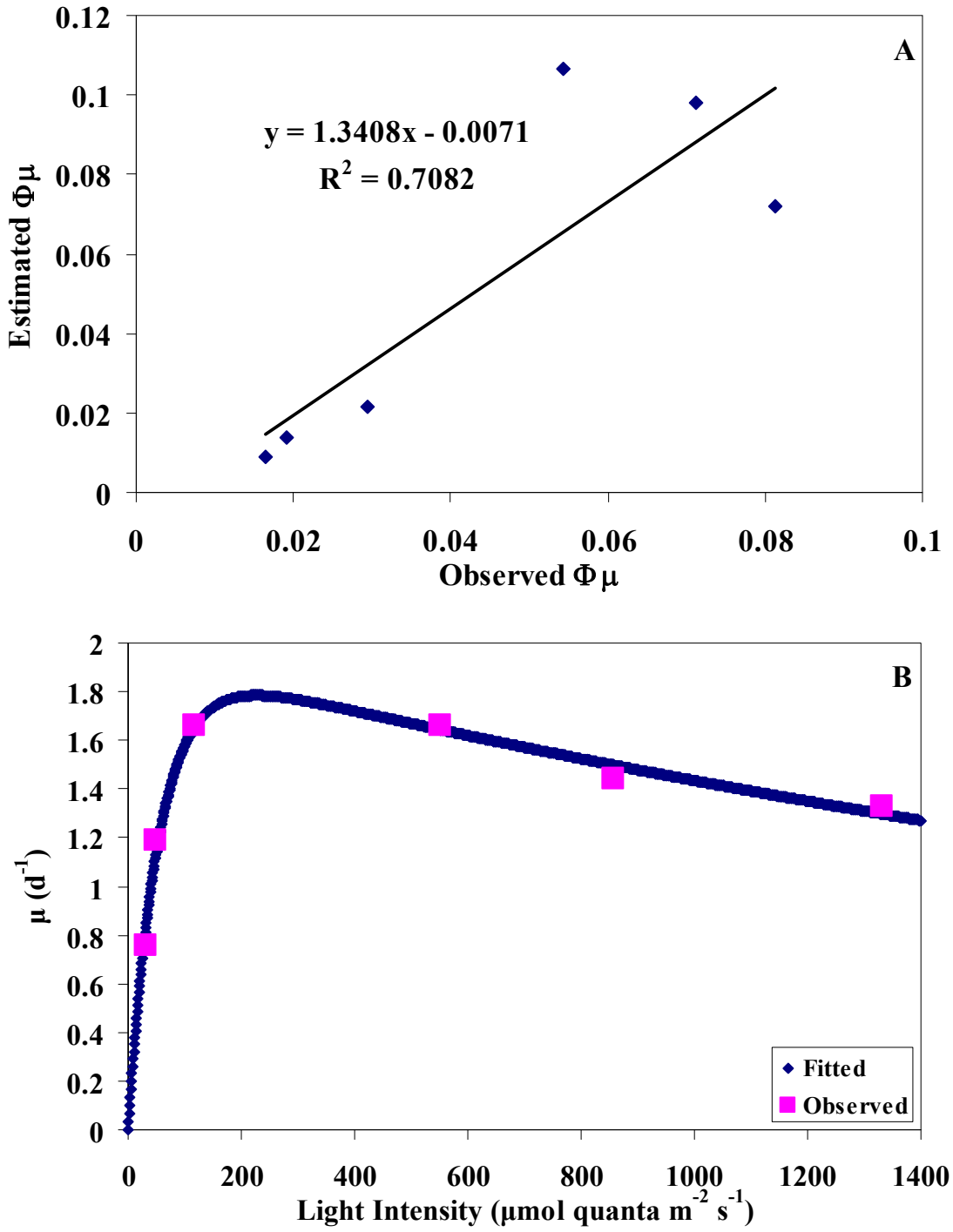

Figure 13. (A) The linear fit between estimated and observed quantum yields (Φ_μ). (B) Non-linear fit of specific growth rates (μ) for *Thalassiosira* used to estimate the saturation irradiance for growth ($E_{k\mu}$).

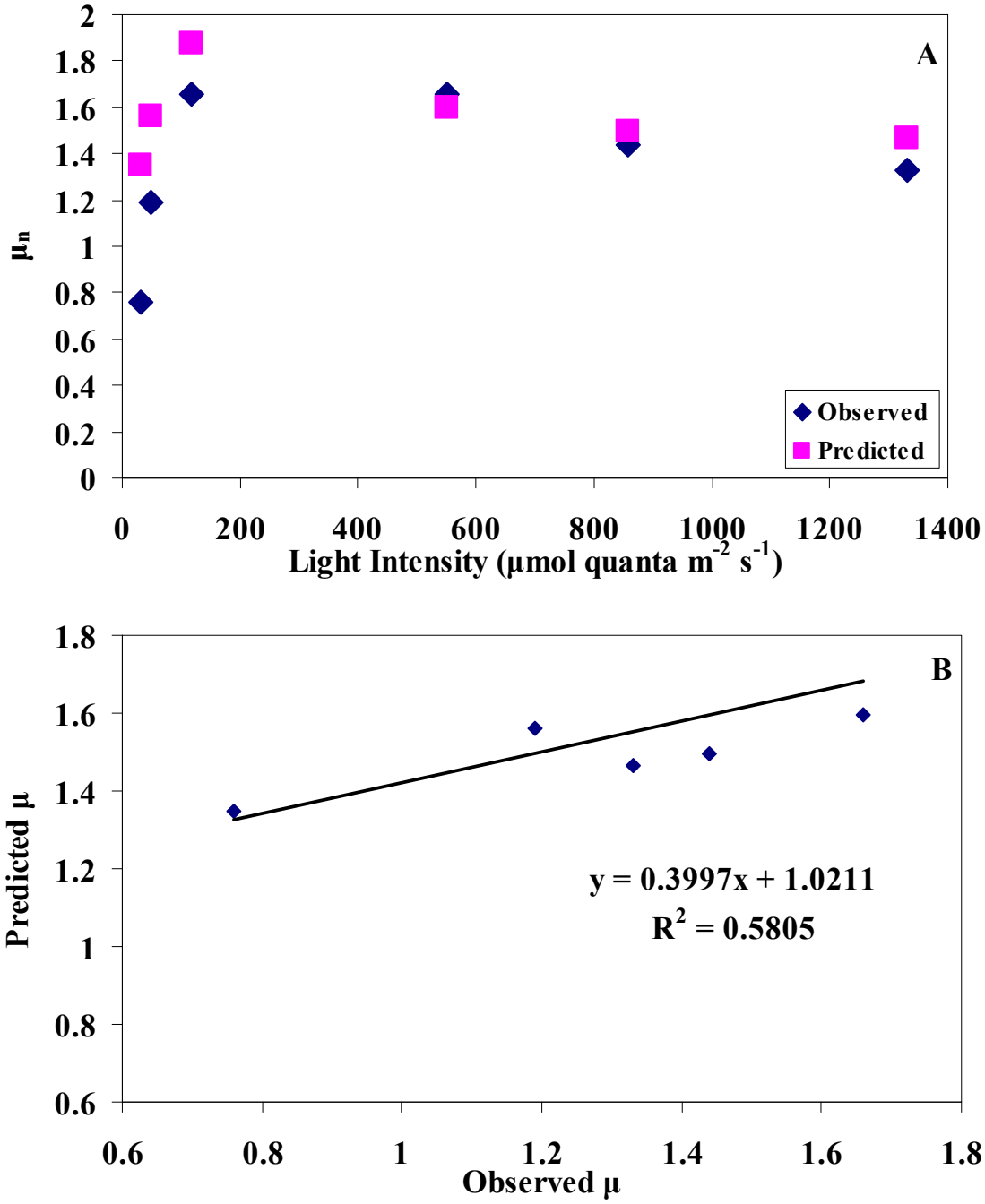

Figure 14. The predicted growth rates, μ, compared to observed growth rates (A) for *Thalassiosira* grown under 31.4, 48.8, 118, 552, 858, and 1332 μmol quanta m^{-2} s^{-1} at 20°C. (B) Linear fit between predicted and observed growth rates.

REFERENCES

1. Armbrust, E.V., Berges,J.A., Bowler,C., Green,B.R., Martinez,D., Putnam,N.H., Zhou,S.G., Allen,A.E., Apt,K.E., Bechner,M., Brzezinski,M.A., Chaal,B.K., Chiovitti,A., Davis,A.K., Demarest,M.S., Detter,J.C., Glavina,T., Goodstein,D., Hadi,M.Z., Hellsten,U., Hildebrand,M., Jenkins,B.D., Jurka,J., Kapitonov,V.V., Kroger,N., Lau,W.W.Y., Lane,T.W., Larimer,F.W., Lippmeier,J.C., Lucas,S., Medina,M., Montsant,A., Obornik,M., Parker,M.S., Palenik,B., Pazour,G.J., Richardson,P.M., Rynearson,T.A., Saito,M.A., Schwartz,D.C., Thamatrakoln,K., Valentin,K., Vardi,A., Wilkerson,F.P., and Rokhsar,D.S. 2004. The genome of the diatom Thalassiosira pseudonana: Ecology, evolution, and metabolism. ***Science,*** 306(5693): 79-86.

2. Benemann, J.R., Van Olst, J,C,, Massingill, M.J., Weissman, J.C., Brune, D.E. 2003. ***The Controlled Eutrophication Process: Using Microalgae for CO2 Utilization and Agricultural Fertilizer Recycling***. Paper presented at the Greenhouse gas control technologies—6th international conference. Oxford: Pergamon.

3. Berner, T., Dubinsky,Z., Wyman,K., and Falkowski,P.G. 1989. Photoadaptation and the Package Effect in Dunaliella-Tertiolecta (Chlorophyceae). ***Journal of Phycology,*** 25(1): 70-78.

4. Bricaud, A., Babin,M., Morel,A., and Claustre,H. 1995. Variability in the Chlorophyll-Specific Absorption-Coefficients of Natural Phytoplankton - Analysis and Parameterization. ***Journal of Geophysical Research-Oceans,*** 100(C7): 13321-13332.

5. Brown, M.R., Dunstan,G.A., Norwood,S.J., and Miller,K.A. 1996. Effects of harvest stage and light on the biochemical composition of the diatom Thalassiosira pseudonana. ***Journal of Phycology,*** 32(1): 64-73.

6. Burris, J.E. 1977. Photosynthesis, Photorespiration, and Dark Respiration in 8 Species of Algae. ***Marine Biology,*** 39(4): 371-379.

7. Chai, C., Yu,Z.M., Song,X.X., and Cao,X.H. 2006. The status and characteristics of eutrophication in the Yangtze River (Changjiang) estuary and the adjacent East China Sea, China. ***Hydrobiologia,*** 563: 313-328.

8. Chen, C.S., Zhu,J.R., Beardsley,R.C., and Franks,P.J.S. 2003. Physical-biological sources for dense algal blooms near the Changjiang River. ***Geophysical Research Letters,*** 30(10)

9. Davis, C.C. 1955. ***The Marine and Fresh-water Plankton***. East Lansing: Michigan State University Press.

10. Demaster, D.J. 1979. ***The Marine Budgets of Silica and ^{32}Si***. Unpublished thesis, Yale University, New Haven.

11. Dubinsky, Z., Falkowski,P.G., and Wyman,K. 1986. Light Harvesting and Utilization by Phytoplankton. ***Plant and Cell Physiology,*** 27(7): 1335-1349.

12. Falkowski, P.G., Dubinsky,Z., and Wyman,K. 1985. Growth-Irradiance Relationships in Phytoplankton. ***Limnology and Oceanography,*** 30(2): 311-321.

13. Falkowski, P.G., Raven, J.A. 2007. ***Aquatic Photosynthesis*** (2nd ed.). Princeton and Oxford: Princeton University Press.

14. Fitton, J.H., Irhimeh, M.R., Teas, J. 2008. Marine Algae and Polysaccharides with Therapeutic Applications. In C. Barrow and F. Shahidi (Eds.), ***Marine Nutraceuticals and Functional Foods:*** 345–361 Boca Raton: CRC Press.

15. Foyer, C.H., Lelandais,M., and Kunert,K.J. 1994. Photooxidative Stress in Plants. ***Physiologia Plantarum,*** 92(4): 696-717.

16. Friedman, A.L. and Alberte,R.S. 1984. A Diatom Light-Harvesting Pigment-Protein Complex - Purification and Characterization. ***Plant Physiology,*** 76(2): 483-489.

17. Groffman, P.M., Law,N.L., Belt,K.T., Band,L.E., and Fisher,G.T. 2004. Nitrogen fluxes and retention in urban watershed ecosystems. ***Ecosystems,*** 7(4): 393-403.

18. Guillard, R.R. and Ryther,J.H. 1962. Studies of Marine Planktonic Diatoms .1. Cyclotella Nana Hustedt, and Detonula Confervacea (Cleve) Gran. ***Canadian Journal of Microbiology,*** 8(2): 229-&.

19. Guillard, R.R. and Lorenzen,C.J. 1972. Yellow-Green Algae with Chlorophyllide C. ***Journal of Phycology,*** 8(1): 10-&.

20. He, P.M., Xu,S.N., Zhang,H.Y., Wen,S.S., Dai,Y.J., Lin,S.J., and Yarish,C. 2008. Bioremediation efficiency in the removal of dissolved inorganic nutrients by the red seaweed, Porphyra yezoensis, cultivated in the open sea. ***Water Research,*** 42(4-5): 1281-1289.

21. Herzig, R. and Falkowski,P.G. 1989. Nitrogen Limitation in Isochrysis-Galbana (Haptophyceae) .1. Photosynthetic Energy-Conversion and Growth Efficiencies. ***Journal of Phycology,*** 25(3): 462-471.

22. Holmhansen, O. and Riemann,B. 1978. Chlorophyll A Determination - Improvements in Methodology. ***Oikos,*** 30(3): 438-447.

23. Howarth, R.W. and Marino,R. 2006. Nitrogen as the limiting nutrient for eutrophication in coastal marine ecosystems: Evolving views over three decades. ***Limnology and Oceanography,*** 51(1): 364-376.

24. Huo, Y.Z., He, P.M., Xu, S.N., Tian, Q.T., Wang, Y.Y., Wu, W.N., Chen, Y.Q. 2010. Bioremediation efficiencies of Gracilaria verrucosa cultivations in an enclosed sea area of Hangzhou Bay, China. Working paper, Shanghai Ocean University College of Fisheries and Life Sciences, Shanghai, China.

25. Jassby, A.D. and Platt,T. 1976. Mathematical Formulation of Relationship Between Photosynthesis and Light for Phytoplankton. ***Limnology and Oceanography,*** 21(4): 540-547.

26. Kiefer, D.A. and Mitchell,B.G. 1983. A Simple, Steady-State Description of Phytoplankton Growth Based on Absorption Cross-Section and Quantum Efficiency. ***Limnology and Oceanography,*** 28(4): 770-776.

27. Laws, E.A. and Bannister,T.T. 1980. Nutrient-Limited and Light-Limited Growth of Thalassiosira-Fluviatilis in Continuous Culture, with Implications for Phytoplankton Growth in the Ocean. ***Limnology and Oceanography,*** 25(3): 457-473.

28. Liu, S.M., Zhang,J., Chen,H.T., Wu,Y., Xiong,H., and Zhang,Z.F. 2003. Nutrients in the Changjiang and its tributaries. ***Biogeochemistry,*** 62(1): 1-18.

29. Mantoura, R.F.C. and Llewellyn,C.A. 1983. The Rapid-Determination of Algal Chlorophyll and Carotenoid-Pigments and Their Breakdown Products in Natural-Waters by Reverse-Phase High-Performance Liquid-Chromatography. ***Analytica Chimica Acta,*** 151(2): 297-314.

30. Mas, S., Roy,S., Blouin,F., Mostajir,B., Therriault,J.C., Nozais,C., and Demers,S. 2008. Diel variations in optical properties of Imantonia rotunda (haptophyceae) and Thalassiosira pseudonana (Bacillariophyceae) exposed to different irradiance levels. ***Journal of Phycology,*** 44(3): 551-563.

31. Mayo, A.W. 1997. Effects of temperature and pH on the kinetic growth of unialga Chlorella vulgaris cultures containing bacteria. ***Water Environment Research,*** 69(1): 64-72.

32. McGarry, M.G. and Tongkasame,C. 1971. Water Reclamation and Algae Harvesting. ***Journal (Water Pollution Control Federation),*** 43(5): 824-835.

33. Mitchell, B.G. and Kiefer,D.A. 1988. Chlorophyll-Alpha Specific Absorption and Fluorescence Excitation-Spectra for Light-Limited Phytoplankton. ***Deep-Sea Research Part A-Oceanographic Research Papers,*** 35(5): 639-663.

34. Moisan, T.A. and Mitchell,B.G. 1999. Photophysiological acclimation of Phaeocystis antarctica Karsten under light limitation. ***Limnology and Oceanography,*** 44(2): 247-258.

35. Moisan, T.A. and Mitchell,B.G. 2001. UV absorption by mycosporine-like amino acids in Phaeocystis antarctica Karsten induced by photosynthetically available radiation. ***Marine Biology,*** 138(1): 217-227.

36. Nelson, D.M., Treguer,P., Brzezinski,M.A., Leynaert,A., and Queguiner,B. 1995. Production and Dissolution of Biogenic Silica in the Ocean - Revised Global Estimates, Comparison with Regional Data and Relationship to Biogenic Sedimentation. ***Global Biogeochemical Cycles,*** 9(3): 359-372.

37. Olguin, E.J. 2003. Phycoremediation: key issues for cost-effective nutrient removal processes. ***Biotechnology Advances,*** 22(1-2): 81-91.

38. Olson, R.J., Soohoo,J.B., and Kiefer,D.A. 1980. Steady-State Growth of the Marine Diatom Thalassiosira-Pseudonana - Uncoupled Kinetics of Nitrate Uptake and Nitrite Production. ***Plant Physiology,*** 66(3): 383-389.

39. Oswald, W.J., Gotaas,H.B., Golueke,C.G., and Kellen,W.R. 1957. Algae in Waste Treatment. ***Sewage and Industrial Wastes,*** 29(4): 437-455.

40. Park, K.Y., Lim,B.R., and Lee,K. 2009. Growth of microalgae in diluted process water of the animal wastewater treatment plant. ***Water Science and Technology,*** 59(11): 2111-2116.

41. Parker, M.S., Armbrust,E.V., Piovia-Scott,J., and Keil,R.G. 2004. Induction of photorespiration by light in the centric diatom Thalassiosira weissflogii (Bacillariophyceae): Molecular characterization and physiological consequences. ***Journal of Phycology,*** 40(3): 557-567.

42. Platt, T., Gallegos,C.L., and Harrison,W.G. 1980. Photoinhibition of Photosynthesis in Natural Assemblages of Marine-Phytoplankton. ***Journal of Marine Research,*** 38(4): 687-701.

43. Rhee,G.Y. and Gotham,I.J. 1981. The Effect of Environmental-Factors on Phytoplankton Growth - Temperature and the Interactions of Temperature with Nutrient Limitation. ***Limnology and Oceanography,*** 26(4): 635-648.

44. Sakshaug, E., Andresen,K., and Kiefer,D.A. 1989. A Steady-State Description of Growth and Light-Absorption in the Marine Planktonic Diatom Skeletonema-Costatum. ***Limnology and Oceanography,*** 34(1): 198-205.

45. Sakshaug, E., Johnsen,G., Andresen,K., and Vernet,M. 1991. Modeling of Light-Dependent Algal Photosynthesis and Growth - Experiments with the Barents Sea Diatoms Thalassiosira-Nordenskioeldii and Chaetoceros-Furcellatus. ***Deep-Sea Research Part A-Oceanographic Research Papers,*** 38(4): 415-430.

46. Sanchez, S., Martinez,E., and Espinola,F. 2000. Biomass production and biochemical variability of the marine microalga Isochrysis galbana in relation to culture medium. ***Biochemical Engineering Journal,*** 6(1): 13-18.

47. Sosik, H.M. and Mitchell,B.G. 1991. Absorption, Fluorescence, and Quantum Yield for Growth in Nitrogen-Limited Dunaliella-Tertiolecta. ***Limnology and Oceanography,*** 36(5): 910-921.

48. Sosik, H.M. and Mitchell,B.G. 1995. Light absorption by phytoplankton, photosynthetic pigments and detritus in the California current system. ***Deep-Sea Research Part I-Oceanographic Research Papers,*** 42(10): 1717-1748.

49. Sosik, H.M. 1996. Bio-optical modeling of primary production: Consequences of variability in quantum yield and specific absorption. ***Marine Ecology-Progress Series,*** 143(1-3): 225-238.

50. Surface Water Quality Standards—GB3838-2002. State Environmental Protection Administration of China. http://www.nthb.cn/standard/standard02/20030428174340.html. June 2010.

51. Valenzuela-Espinoza, E., Millan-Nunez,R., and Nunez-Cebrero,F. 1999. Biomass production and nutrient uptake by Isochrysis aff. galbana (Clone T-ISO) cultured with a low cost alternative to the f/2 medium. ***Aquacultural Engineering,*** 20(3): 135-147.

52. Valenzuela-Espinoza, E., Millan-Nunez,R., Trees,C.C., Santamaria-del-Angel,E., and Nunez-Cebrero,F. 2007. Growth and accessory pigment to chlorophyll a ratios of Thalassiosira pseudonana (Bacillariophyceae) cultured under different irradiances. ***Hidrobiologica,*** 17(3): 249-255.

53. Varis, O. and Vakkilainen,P. 2001. China's 8 challenges to water resources management in the first quarter of the 21st Century. ***Geomorphology,*** 41(2-3): 93-104.

54. Water Quality Assessment of the Condition of California Coastal Waters and Wadeable Streams. Clean Water Act Section 305b Report 2006. http://www.swrcb.ca.gov/water_issues/programs/swamp/docs/factsheets/305breport2006.pdf. June 2010.

55. Woertz, I., Feffer,A., Lundquist,T., and Nelson,Y. 2009. Algae Grown on Dairy and Municipal Wastewater for Simultaneous Nutrient Removal and Lipid Production for Biofuel Feedstock. ***Journal of Environmental Engineering-Asce,*** 135(11): 1115-1122.

56. Wu, J.Y. 2005. Assessing surface water quality of the Yangtze Estuary with genotoxicity data. ***Marine Pollution Bulletin,*** 50(12): 1661-1667.

57. Yang, Y.F., Fei,X.G., Song,J.M., Hu,H.Y., Wang,G.C., and Chung,I.K. 2006. Growth of Gracilaria lemaneiformis under different cultivation conditions and its effects on nutrient removal in Chinese coastal waters. ***Aquaculture,*** 254(1-4): 248-255.

58. Yoshida, T., Hairston,N.G., and Ellner,S.P. 2004. Evolutionary trade-off between defence against grazing and competitive ability in a simple unicellular alga, Chlorelia vulgaris. ***Proceedings of the Royal Society of London Series B-Biological Sciences,*** 271(1551): 1947-1953.

59. Zhou, M.J., Shen,Z.L., and Yu,R.C. 2008. Responses of a coastal phytoplankton community to increased nutrient input from the Changjiang (Yangtze) River. ***Continental Shelf Research,*** 28(12): 1483-1489.